



2nd Nuclear Technologies for Health Symposium

February 12 - 14, 2014

Nantes, France



CONTENT

Committees	p4
Welcoming words	p5
Acknowledgements	p6
General information	p8
Scientific program	p10
Abstracts	p16
List of participants	p62



2nd Nuclear Technologies for Health Symposium

February 12 - 14, 2014

Nantes, France

A photograph of the Nantes skyline, featuring the dome of St. Pierre Cathedral, viewed through a large circular frame made of metal rings. The foreground shows a river and a rusty metal railing.

FINAL PROGRAM

SCIENTIFIC COMMITTEE

Jacques Barbet
Jean-Pierre Benoit
Myriam Bernaudin
Thomas Carlier
Michel Chérel
Nicolas Chouin
Alain Faivre-Chauvet
Jean-François Gestin
Denis Guilloteau
Françoise Kraeber-Bodéré
Gilles Montavon

LOCAL ORGANIZING COMMITTEE

Jacques Barbet
Stéphanie Desevedavy
Marie-Hélène Gaugler
Françoise Kraeber-Bodéré
Djamila Mérouani

ORGANIZATION



WELCOMING WORDS

Dear colleagues,

It is our pleasure to welcome you to the second edition of the Nuclear Technologies for Health Symposium (NTHS) in Nantes, France, from 12 to 14 February 2014. The symposium is hosted by the *Nuclear Technologies for Health* (NucSan) project sponsored by the Pays de la Loire Regional Council and by the *Innovative Radiopharmaceuticals in Oncology and Neurology* (IRON) *Laboratory of Excellence* (LabEx) project sponsored by the French government.

These two multidisciplinary projects aim at developing nuclear medicine tools for personalized medicine in neurology and oncology, by the transfer to the clinic of innovative radiopharmaceuticals produced by a cyclotron network involving Arronax (Nantes), Cyrce (Strasbourg), Cyceron (Caen), PET Center (Toulouse) and CERRP (Tours). In this context, it is essential to reinforce the dialogue between researchers of different backgrounds, from nuclear physics to medicine, including chemistry, biology and many other disciplines.

These projects also aim at establishing strong partnerships with industry and offering innovative teaching and training programs around the production of radiopharmaceuticals.

The local Organizing Committee and the NTHS Scientific Committee have worked together to prepare a program that will include the latest developments in the fields of neurological disease imaging, tumor imaging, radionuclide targeted therapy and related topics, together with timely reviews presented by outstanding plenary speakers.

The NTHS meeting remains a unique opportunity to bring together the various actors in these fields and is of interest to both junior and senior basic scientists, as well as clinical researchers and practitioners. The meeting promotes interactions between these different groups.

On behalf of the Organizing Committee, we welcome you to Nantes. We are delighted that you joined us for the NTHS 2014 - a stimulating meeting offering enjoyable and rewarding interactions between basic and clinical researchers in the fields of neurological disease imaging, tumor imaging, radionuclide targeted therapy and related topics.

Jacques Barbet
Leader of the NucSan project

Françoise Kraeber-Bodéré
Leader of the IRON LaBex project

ACKNOWLEDGEMENTS

The Organizing Committee would like to express their sincere appreciation to the following organisations for their support in the 2nd Nuclear Technologies for Health Symposium.

SPONSORS



Bayer HealthCare



LEMER PAX
I N N O V A T I V E



inviscan
Imaging systems

DOSI  soft



EXHIBITORS



Bayer HealthCare



SPECTRUMTM

PHARMACEUTICALS

Redefining Cancer Care



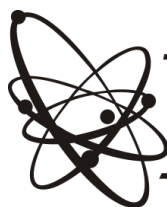
GE Healthcare



DOSI  soft

inviscan

Imaging systems



raytest

INSTITUTIONAL SUPPORT



UNIVERSITÉ DE NANTES



Région

PAYS DE LA LOIRE



GENERAL INFORMATION

VENUE

CCI Nantes St-Nazaire

Centre des Salorges

16 quai Ernest Renaud Nantes

Tel. No 33(0) 2 40 44 60 00

Tram station « Gare Maritime » line 1 direction : François Mitterand

ON SITE REGISTRATION DESK OPENING

Wednesday, Feb 12, 08:00 - 18:00

Thursday, Feb 13, 08:00 - 18:00

Friday, Feb 14, 08:00 - 15:00

LANGUAGE

English is the official language of the Symposium. All presentations will be made in English.

INSTRUCTIONS FOR PRESENTERS

Please note that you need to bring your power point presentation on a « disk on key » memory stick and load it on the computer of the symposium (PC, power point 2010) during a coffee or lunch break prior to your session. No private computer will be allowed.

INSTRUCTIONS FOR POSTER PRESENTERS

Posters will be on display for the entire symposium (installation : wednesday, feb 12 before 10:00 and removal friday, feb 14 before 16:00). Presenters are requested to stand next to their posters thursday, feb 13, 09:00 - 09:45. Poster sessions will occur during coffee breaks and lunches.

WIFI

ID : NTHS

Password : NTHS

SYMPOSIUM DINNER (for registered only)

Thursday, February 13, 20:00

Le Square

14 rue de Jemmapes

44000 Nantes

Tel : 02 40 35 98 09



SCIENTIFIC PROGRAM



08:30 - 09:45 Registration and welcome coffee

Opening ceremony

10:00 Opening and welcome **Pr Françoise Kraeber-Bodéré, Dr Jacques Barbet**

10:30 **Pr Andreas Jacobs** (European Institute for Molecular Imaging, Germany)
Molecular imaging for assessment of treatment response in patients with glioma

Session 1: Targeted radionuclide therapy

Chairs: Pr Françoise Kraeber-Bodéré, Pr Jean-Pierre Benoit

11:15 **Pr Wim Oyen** (Radboud University Medical Centre, The Netherlands)
Targeted radionuclide therapy using monoclonal antibodies and related products

12:00 - 13:30 Lunch and posters

13:30 **Vincent Boudousq** (IRCM/Inserm U896, Montpellier, France)
Anti-CEA versus anti-HER2 ²¹²Pb-labeled mAbs in α -RIT of small volume peritoneal carcinomatosis - Dose effect relationship?

13:50 **Aurélien Derrien** (CRCNA, UMR 892 Inserm - 6299 CNRS, Nantes, France)
Evaluation in nude mice of Targeted Alpha-Therapy with Bismuth-213 versus Heated Intraoperative Intraperitoneal Chemotherapy

14:10 **Jean-Baptiste Gorin** (CRCNA, UMR 892 Inserm - 6299 CNRS, Nantes, France)
Anti-tumour immunity induced after alpha irradiation

14:30 **Jérémy Ménager** (CRCNA, UMR 892 Inserm - 6299 CNRS, Nantes, France)
Adoptive T cell therapy potentiates efficacy of alpha radio-immunotherapy

14:50 - 15:20 Coffee break and posters

15:20 **Delphine Séhédic** (MINT, UMR 1066 Inserm, Angers, France)
Development of new nanocarriers for alpha and beta targeted radiotherapy in glioblastoma

15:40 **Mathias Tesson** (ICS, University of Glasgow, UK)
Enhancement of prostate-targeted radiotherapy using [¹³¹I]MIP-1095 in combination with radiosensitizing chemotherapeutic drugs

16:00 **Irini Baka** (Department of Radiology, Aretaieion Hospital, Athens, Greece)
The role of Patient Specific Dosimetry after Peptide Receptor Radionuclide Therapy (PRRT) with Lutetium-177 [¹⁷⁷Lu - DOTA⁰, Tyr³] octreotate

16:20 **Amandine Pallardy** (CHU/ICO/CRCNA, Nantes, France)
Consolidation Anti-CD22 Fractionated Radioimmunotherapy (RIT) with 90Y-Epratuzumab Tetraxetan Following R-CHOP in Elderly Diffuse Large B-cell Lymphoma (DLBCL) Patients

16:40 End of the session

09:00 Poster presentations

Session 2: Functional and phenotype imaging

Chairs: Pr Denis Guilloteau, Pr Michel Chérel

09:45 **Matthieu Bailly** (CHU, Tours, France)
Regional analysis of ^{18}F -FDG and ^{18}F -Florbetapir PET in elderly, mild cognitive impairment and Alzheimer's disease

10:05 **Sylvie Chalon** (UMR 930 Inserm, Tours, France)
In vivo PET quantification of the dopamine transporter in rat brain with [^{18}F]LBT-999 and application in a rat model of Parkinson's disease

10:25 - 10:55 Coffee break and posters

10:55 **Amandine Pallardy** (CHU/ICO/CRCNA, Nantes, France)
Relationship between clinical features of Lewy pathology and dopaminergic function throughout the Alzheimer Disease Dementia with Lewy bodies spectrum

11:15 **Charles-Henri Malbert** (ADNC, Saint-Gilles, France)
Early changes in brain metabolism following vagal stimulation

11:35 **Maria-Joao Santiago-Ribeiro** (CHU/CIC-IT/UMR 930 Inserm, Tours, France)
Relationship between β -amyloid density and cortical perfusion in Posterior Cortical Atrophy and Progressive Primary Aphasia

11:55 **Maria-Joao Santiago-Ribeiro** (CHU/CIC-IT/UMR 930 Inserm, Tours, France)
Brain kinetics of ^{18}F -DPA-714 in acute and chronic neuroinflammation

12:15 - 13:45 Lunch and posters

13:45 **Dr Lisa Bodei** (European Institute of Oncology, Italy)
Peptides in nuclear medicine for PET and molecular radiotherapy

14:30 **Olivier Couturier** (CHU, Angers, France)
3'-Fluorine-18-3'-deoxy-L-Thymidine (FLT) positron emission tomography (PET): an accurate and effective tool for assessing tumor response in breast cancer

14:40 **Aurélien Corroyer-Dulmont** (ISTCT UMR 6301 CNRS, Caen, France)
Assessment of hypoxia with 3- ^{18}F -fluoro-1-(2-nitro-1-imidazolyl)-2-propanol ([^{18}F]-FMISO): a noninvasive tool to improve treatment efficacy in GBM

15:10 - 15:40 Coffee break and posters

- 15:40** **Cédric Mathieu** (CHU, Nantes, France)
⁶⁸Ga-DOTANOC PET/CT in well-differentiated gastro-enteropancreatic neuroendocrine tumors (GEP-TNEs): prospective comparison with somatostatin receptor SPECT/CT and four-phase CT; preliminary results
- 16:00** **Etienne Matous** (CRCNA, UMR 892 Inserm - 6299 CNRS, Nantes, France)
Development of Affitins for tumor targeting
- 16:20** **Narinée Hovhannisyan** (ISTCT UMR 6301 CNRS, Caen, France)
A quantitative evaluation of the influence of Rituximab therapy and tumor growth on 2-[¹⁸F]Fludarabine uptake by PET/CT imaging in a follicular lymphoma xenograft model
- 16:40** **Caroline Rousseau** (CHU/ICO/CRCNA, Nantes, France)
Feasibility of pretargeted immuno-PET using an anti-CEA bispecific antibody and a ⁶⁸Ga-labeled hapten-peptide in metastatic breast and medullary thyroid carcinoma patients: preliminary results
- 17:00** End of the session

20:00 symposium dinner

Session 3: Innovations in Radiochemistry, Chemistry and Radiopharmacy

Chairs: Dr Jean-François Gestin, Dr Gilles Montavon

- 08:30** Dr Sergio Todde (Milano-Bicocca University, Italy)
GMP issues of automated systems for radiopharmaceutical preparations
- 08:55** Julie Champion (Subatech, Nantes, France)
Investigation of astatine chemistry in solution
- 09:15** Damien Cressier (ISTCT, Caen, France)
Radiolabelling and evaluation of [⁶⁸Ga]PIB derivatives for Alzheimer's disease diagnostic
- 09:35** Fabienne Gourand (ISTCT, Caen, France)
Chemical delivery system of tracers to the central nervous system (CNS)

09:55 - 10:25 Coffee break and posters

- 10:25** Dr Cécile Pérrio (Cyceron, France)
Microfluidic contributions on fluorine radiochemistry
- 10:50** Cécile Pérrio (ISTCT, Caen, France)
Synthesis of 4-([¹⁸F]fluoromethyl)piperidines for PET imaging
- 11:10** Magali Szlosek-Pinaud (ISM, Bordeaux, France)
In the way to the quest of « the ideal » [¹⁸F]-radiotracer targeting tumor neoangiogenesis: from the chemistry to the imaging of $\alpha_v\beta_3$ integrins in melanoma tumors
- 11:30** Johnny Vercouillie (UMR 930 Inserm, Tours, France)
A novel radiotracer to image alpha 7 by PET, the [¹⁸F] FP321
- 11:50** Nicolas Arlicot (UMR 930 Inserm, Tours, France)
Imaging tumor matrix microenvironment by PET with a fluorinated heparansulfate mimetic

12:10 - 13:10 Lunch and posters

Session 4: Quantitative imaging and absorbed dose/biological effect relationship

Chairs: Dr Thomas Carlier, Dr Nicolas Chouin

- 13:10** Dr Stig Palm (Gothenburg University, Sweden)
Quantitative imaging, biokinetic modeling and Monte Carlo radiation transport methods for Astatine-211 micro-, small- scale and patient-organ dosimetry
- 13:55** Ludovic Ferrer (CHU/ICO/CRCNA, Nantes, France)
Absorbed doses estimations for patients with B-acute lymphoblastic leukemia treated by radioimmunotherapy ⁹⁰Y-epratuzumab tetraxetan
- 14:15** Etienne Garin (CEM, Rennes, France)
Boosted selective internal radiation therapy (B-SIRT) using ⁹⁰Y-loaded glass microspheres induces prolonged overall survival for PVT patients

14:35 - 14:50 Coffee break

- 14:50** Manuel Sanchez-Garcia (Beaujon Hospital, Clichy, France)
Collapsed cone superposition for radionuclide dosimetry: implementation and validation for ⁹⁰Y therapy
- 15:10** Matthieu Moreau (CRCNA, Oniris, Nantes, France)
Development of a fully 3D Monte Carlo reconstruction method for Preclinical PET with Iodine-124 (ReS_PET): efficiency in heterogeneous media
- 15:30** Henri Der Sarkissian (IRCCyN, Nantes, France)
Comparative study of tomographic reconstructions algorithms for dosimetry purposes

15:50 - 16:10 Poster and oral presentation awards ceremony

- 16:15** End of the symposium



ABSTRACTS



Oral presentation

Anti-CEA *versus* anti-HER2 ^{212}Pb -labeled mAbs in α -RIT of small volume peritoneal carcinomatosis – Dose effect relationship?

Alexandre Pichard¹, Vincent Boudousq¹, Laure Bobyk¹, Riad Ladjohounlou¹, Salomé Paillas¹, Marion Le Blay¹, Muriel Busson¹, Catherine Lozza¹, Patrick Maquaire², Julien Torgue³, Isabelle Navarro-Teulon¹ and Jean-Pierre Pouget¹

¹IRCM/INSERM U896 Montpellier, France

²AREVA NC, Beaumont-Hague, France

³AREVA Med, 7475 Wisconsin Ave, Bethesda, MD 20814, USA

Jean-pierre.pouget@inserm.fr

Hypothesis: We compared the anti-tumor efficacy and toxicity of non-internalizing (anti-CEA) or internalizing (anti-HER2) ^{212}Pb -labeled mAbs during alpha-radioimmunotherapy of small volume peritoneal carcinomatosis. The relationship between tissue absorbed doses and biological endpoints was also assessed.

Methods: Mice bearing intraperitoneal (i.p.) A-431 tumor cells xenografts (2–3 mm) were i.p. injected with increasing activities (370–1480 kBq; 37 MBq/mg) of either 35A7 (anti-CEA), Trastuzumab (anti-HER2) or PX (non-specific) ^{212}Pb -labeled mAbs. Control groups were injected with corresponding amount of unlabeled mAbs or with NaCl. Tumor growth was monitored by bioluminescence and median survival (MS) of control and treated mice was determined. ^{212}Pb -35A7 and ^{212}Pb -Trastuzumab biodistribution was used to determine the cumulative uptake of radioactivity (UOR) in organs and tumors. Mean absorbed doses were calculated using the MIRD formalism. Hematological, liver and kidney toxicities were also assessed. Distribution of radioactivity was also determined at the tissue level using digital micro-autoradiography for subsequent dose distribution.

Results: Hematological toxicity was observed in groups treated with the highest amount of activity but was shown to be mild and transient. MS of the groups treated either with internalizing or non-internalizing ^{212}Pb -labeled mAbs was significantly improved compared to those treated with non-specific ^{212}Pb -PX or those only given unlabeled mAbs or just NaCl. MS ranged from 42 d to 94 d using various activity levels of anti-CEA ^{212}Pb -35A7 while MS was not reached over the follow-up period of 130 d for mice treated with anti-HER2 ^{212}Pb -Trastuzumab. However, UOR and absorbed doses were shown to be higher for ^{212}Pb -35A7 mAb than for ^{212}Pb -Trastuzumab (35.5 Gy versus 27.6 Gy, respectively). Investigation of potential relationships between distribution of radioactivity and subsequent dose distribution at the tissue level and biological parameters is ongoing.

Conclusions: We showed the strong therapeutic efficacy of ^{212}Pb -labeled mAbs in i.p. α -RIT of small volume tumors. Internalizing ^{212}Pb -labeled mAbs were the most efficient although tumor absorbed dose was lower than for non-internalizing ^{212}Pb -labeled mAbs. Such a lack of absorbed dose/effect relationship could be explained by differential heterogeneous distribution of the two radiolabeled mAbs or by the involvement of bystander effects.

Oral presentation

Evaluation in nude mice of Targeted Alpha-Therapy with Bismuth-213 versus Heated Intraoperative Intraperitoneal Chemotherapy

Aurélie Derrien^{1,2,3}, Michel Chérel^{1,2,3,4}, Sébastien Gouard^{1,2,3}, Catherine Maurel^{1,2,3}, Sandrine Minault^{1,2}, Jean-Marc Classe⁵.

¹ INSERM, U892 – CRCNA, Nantes, France

² Université de Nantes, Nantes, France

³ CNRS UMR 6299, Nantes, France

⁴ Institut de Cancérologie de l'Ouest, Saint-Herblain, France

⁵ Department of Oncologic Surgery, Institut de Cancérologie de l'Ouest, Saint-Herblain, France.

Objectives: Ovarian carcinoma is a pathology for which efficient cures are currently lacking. New research protocols intend to eradicate micrometastasis by using Hyperthermic Intraperitoneal Chemotherapy (HIPEC) after cytoreductive surgery, or Radioimmunotherapy (RIT). This study first aims at developing a new α -RIT technique using 213-Bismuth, and secondly, at comparing and associating that technique with HIPEC in a Nude mice model.

Methods and Results: A human ovarian carcinoma cell line (SHIN-3) was used. SHIN-3 cells express CD138 and were transduced to express Luciferase (Luc). We confirmed that CD138 expression as well as growth was not significantly modified in transduced cells (SHIN-3-Luc) compared to parental cells SHIN-3. We primarily analyzed the effect of Bi-labeled BB4 combined with hyperthermia in vitro using the Clonogenic assay. For a 60 minute exposure, the 50% lethal dose (LD50) was equivalent between 37 and 40°C. Then, we established a murine model of metastatic epithelial ovarian cancer by intraperitoneal injection of 10^6 SHIN-3-Luc cells into Nude mice. Those mice underwent cytoreductive surgery and their evolution was followed by bioluminescence imaging. In line with this, we developed a murine hyperthermic intraperitoneal chemotherapy model with Cisplatine. Eventually, 22 mice on 24 grafted with 5.10^6 SHIN-3-Luc cells were included and were either treated by HIPEC alone (n=5), α -RIT (n=6), by HIPEC + α -RIT (n=5) or were included in a control group (n=6). Tumor volume, weight, bioluminescence imaging and survival were measured. α -RIT alone inhibited bioluminescence signal (p=0,0004) and was associated with increased survival (p=0,0402). Survival was not significantly different after HIPEC alone or after HIPEC + α -RIT.

Conclusion: Survival was significantly improved by α -RIT with Bismuth-213-BB4 in mice with peritoneal carcinomatosis of ovarian origin. HIPEC alone or HIPEC + α -RIT did not improve survival and was more toxic than α -RIT.

Oral presentation

Anti-tumour immunity induced after alpha irradiation

Jean-Baptiste Gorin^{1,2,3}, Jérémie Ménager^{1,2,3}, Sébastien Gouard^{1,2,3}, Catherine Maurel^{1,2,3}, Yannick Guilloux^{1,2,3}, Alain Faivre-Chauvet^{1,2,3,5}, Alfred Morgenstern⁶, Frank Bruchertseifer⁶, Michel Chérel^{1,2,3,4}, François Davodeau^{1,2,3} and Joëlle Gaschet^{1,2,3}

¹ INSERM UMR 892 - CRCNA, ² University of Nantes, ³ CNRS UMR 6299, Nantes, France

⁴ Institut de Cancérologie de l'Ouest, Saint-Herblain, France

⁵ CHU Nantes, Nuclear medicine department, Nantes, France

⁶ Institute for Transuranium Elements, Karlsruhe, Germany

Objectives: Radioimmunotherapy (RIT) is a therapeutic modality that allows delivering of ionizing radiation directly to targeted cancer cells. Conventional RIT uses beta-emitting radioisotopes, but recently a growing interest has emerged for the clinical development of alpha particles. Alpha emitters are ideal for killing isolated or small clusters of tumour cells, thanks to their high linear energy transfer (LET) and short path in the tissue. So far, no investigation has been undertaken to analyze the impact of alpha particles on the immune system, when several studies have shown that external irradiation, using gamma and X-rays can foster an anti-tumour immune response. Here we investigate the effect of alpha radiation on tumour cell immunogenicity.

Methods: We decided to evaluate the immunogenicity of murine adenocarcinoma MC-38 after bismuth-213 (²¹³Bi) irradiation using a vaccination approach in immunocompetent C57Bl/6 mice. The molecular mechanisms potentially involved in the activation of adaptive immunity were also investigated by *in vitro* studies.

Results: Vaccination induced a protective anti-tumour response that was mediated by tumour specific T cells and we also showed that ²¹³Bi treated MC-38 cells release "danger signals" and activate dendritic cells *in vitro*.

Conclusion: Our results demonstrate that alpha irradiation can stimulate adaptive immunity, elicits an efficient anti-tumour protection and therefore is an immunogenic cell death (ICD) inducer, which provides an attractive complement to its direct cytolytic effect.

Oral presentation

Adoptive T cell therapy potentiates efficacy of alpha radio-immunotherapy.

Jérémie Ménager^{1,2,3}, Jean-Baptiste Gorin^{1,2,3}, Sébastien Gouard^{1,2,3}, Catherine Maurel^{1,2,3}, Michel Chérel^{1,2,3,4}, Alfred Morgenstern⁶, Frank Bruchertseifer⁶, François Davodeau^{1,2,3}, Joëlle Gaschet^{1,2,3} and Yannick Guilloux^{1,2,3}

¹ INSERM, U892 - CRCNA, Nantes, France, ² Université de Nantes, Nantes, France, ³ CNRS UMR 6299, Nantes, France

⁴ Institut de Cancérologie de l'Ouest, Saint-Herblain, France

⁵ CHU Nantes, Nuclear Medicine Department, Nantes, France

⁶ Institute for Transuranium Elements, Karlsruhe, Germany
jeremie.menager@etu.univ-nantes.fr

Hypothesis: Alpha radio-immunotherapy (α -RIT) is a cancer therapy that allows delivery of α radionuclides to tumour cells. α -RIT is currently evaluated in the treatment of different solid as well as disseminated cancers. *In vivo*, investigation of α -RIT mechanisms is rare and very few combined treatments have been performed. Therefore, as for external beam radiotherapy, optimizing α -RIT efficacy may be considered to foster immunity against cancer. Combining α -RIT with adoptive T cell transfer (ACT) is one way to boost the immune system. Multiple myeloma (MM) is a malignant proliferation of plasma cells spreading throughout bone marrow and therefore untreatable with external beam radiation. Despite the evolution of the treatments, this cancer remains incurable and development of new therapies is necessary. Thus, this study aims to investigate the therapeutic association between α -RIT and ACT with tumor specific T lymphocytes to treat MM.

Methods: The therapeutic association is performed in the immunocompetent C57BL/KaLwRij / 5T33 MM mouse model. 5T33 MM cells express CD138 and were transduced to express Ovalbumin (OVA). Thus, α -RIT targets isolated scattered MM cells using an anti-CD138 antibody labelled with bismuth-213, an α emitter. The adoptive transfer consists in the injection of OVA specific CD8⁺ T lymphocytes (OT-I).

Results: We showed that OT-I efficiently recognized 5T33-OVA, *in vitro*. Mice, injected with 5T33-OVA and treated with α -RIT combined with OT-I transfer, demonstrated significant better tumour growth control and improved survival compared to α -RIT or OT-I alone (median survival: 95,5 vs. 68 days for α -RIT alone and 55,5 days for OT-I alone). Monitoring of injected cells showed that OT-I migrate to the tumour site. Only the animals receiving the combined treatment, exhibited stimulation of their immune system, as demonstrated by delayed tumour growth and increased immune cell infiltrates in the tumours.

Conclusion: Altogether, our data demonstrate efficacy of the therapeutic association and a significant impact on the immune system. This preclinical study provides encouraging results to combine ACT of tumour specific T lymphocytes with α -RIT for cancer treatment.

Oral presentation

Development of new nanocarriers for alpha and beta targeted radiotherapy in glioblastoma

Delphine Séhédic¹, Marie Mougin-Degraeff², François Hindré¹, François Davodeau², Emmanuel Garcion¹

¹U1066 MINT, 4 rue Larrey, 49933 ANGERS

²U892 CRCNA, 8 quai Moncousu, 44007 NANTES

delphine.sehedic@etud.univ-angers.fr

Hypothesis: Glioblastoma multiform (GBM) is the most common primary brain tumor in adult with a prevalence of 5 cases/100000 habitants. Current therapy effectiveness is indeed largely limited by resistance mechanisms combining intrinsic properties of tumour cells to the influence of the microenvironment in which they develop (e.g. hypoxia). In this work, we deal to target a radioresistance-associated epitope in GBM cells, the CXCR4, and to develop lipid nanocapsules (LNC) loaded with radionuclides.

Methods: As CXCR4 receptor has been associated with radio-resistance and with cancer stem-like cell (CSLC) occurrence, we focused on the targeting of this protein in a human GBM models (A172, U87MG overexpressing the CXCR4 and human primary GBM cells). We then developed and characterized 50 nm lipid nanocapsules (LNCs) functionalized with a function-blocking monoclonal antibody (mAb) directed against CXCR4 (or isotype control). Those functionalized or function-free LNCs were further combined to ¹⁸⁸Re (beta emitter) and ²¹¹At (α-emitter) for physicochemical evaluation and capability to stably convey the chosen radiopharmaceutics *in vivo*.

Results: By using immunofluorescence flow cytometry, we found that CXCR4 expression is correlated with radiation doses with 10% CXCR4 positive cells in control versus 41% after a 32Gy treatment. Encapsulation of ¹²⁵I (β-emitter and halogen) in miniaturization of the process, which will help for the development of ²¹¹At (halogen), demonstrated its feasibility with a stable encapsulation over time of SIB or more lipophilic SIB-octadécylamine (in C18) in different medium. *In vivo* efficacy of the different systems is under investigation after orthotopic implantation of human GBM cells in immunodeprived SCID mice and loco-regional convective infusion of the radiotherapeutic nano-objects.

Conclusion: Our work combined the interest of targeting CSLC associated epitopes to the one of inhibiting CXCR4 signaling pathways to overcome radioresistance. It also constitutes a pre-requisite for addressing the relevance of β- versus α-nanocarrier radiotherapy in glioblastoma.

SESSION 1 : Targeted radionuclide therapy

Oral presentation

Enhancement of prostate-targeted radiotherapy using [¹³¹I]MIP-1095 in combination with radiosensitizing chemotherapeutic drugs

Tesson M¹, Mairs RJ¹, Joyal JL² and Babich JW³

¹*Institute of Cancer Science, University of Glasgow, Glasgow, United Kingdom.*

²*Moderna Therapeutics, Cambridge, Massachusetts;* ³*Cornell University, New York, Ithaca.*
m.tesson.1@research.gla.ac.uk

Objective : The prostate specific membrane antigen (PSMA)-targeting small molecule radiopharmaceutical, MIP-1095 (J Med Chem 2009, 22; 52(2): 347-57), was radiolabeled with I-131 and evaluated pre-clinically. Growth delay of spheroids derived from LNCaP prostate carcinoma cells was used to determine the radiosensitising potential of various chemotherapeutic drugs in combination with [¹³¹I]MIP-1095.

Method : Enhanced efficacy was manifest by a statistically significant reduction of the area under the volume/time growth curve (AUC) resulting from combination treatment compared with that achieved by either the drug alone or [¹³¹I]MIP-1095 alone. Various chemotherapeutic agents were investigated for synergistic interaction: olaparib (PARP-1 inhibitor), topotecan (topoisomerase I inhibitor), bortezomib (proteasome inhibitor), docetaxel (mitotic spindle-targeting agent), nutlin-3 (inhibitor of the P53-MDM2 interaction) and DSF:Cu (the copper-chelated form of disulfiram).

Results : DSF:Cu showed the greatest radiosensitising effect, indicated by AUC values of 34.59 ± 1.00 for control, 23.53 ± 1.10 for [¹³¹I]MIP-1095, 22.71 ± 1.85 for DSF:Cu and -5.55 ± 1.76 ($P < 0.001$) for the combination of [¹³¹I]MIP-1095 with DSF:Cu. Cell cycle analysis demonstrated that DSF:Cu decreased the G2 population from 25.7% to 18.67% ($P < 0.01$) after gamma-irradiation from a Cobalt-60 source. Synergism between DSF:Cu and gamma-irradiation was also demonstrated in SK-N-BE(2c) (neuroblastoma) and UVW (glioma) cell lines by clonogenic assay in conjunction with isobologram and combination index (CI) analyses. The CI values for combination treatment were 0.71 ± 0.11 for SK-N-BE(2c) and 0.76 ± 0.13 for UVW, indicative of supra-additive clonogenic cell kill.

Conclusions : These results demonstrated that DSF:Cu enhanced the efficacy not only of external beam radiation but also of targeted radionuclide therapy in the form of [¹³¹I]MIP-1095. The suggested mechanism is inhibition of radiation-induced G2 arrest. Therefore disulfiram may have anti-cancer potential in combination with radiotherapy.

Oral presentation

The role of Patient Specific Dosimetry after Peptide Receptor Radionuclide Therapy (PRRT) with Lutetium -177 [^{177}Lu – DOTA⁰,Tyr³] octreotate

I. Baka¹, A. Ploussi¹, M. Argyrou¹, A. Valasi¹, G.Limouris², M.Lyra^{1,2}

¹ Radiation Physics Unit,

² Nuclear Medicine Section,

1st Department of Radiology, Aretaieion hospital, University of Athens

irini_baka@hotmail.com

Objectives: Response and toxicity prediction is essential to the implementation of Peptide Receptor Radionuclide Therapy (PRRT) for neuroendocrine tumors. Radiolabelled somatostatin analogue [^{177}Lu -DOTA⁰, Tyr³] octreotate stands as a promising therapy tool. Specific dosimetry is a crucial factor in patient treatment planning. Dosimetric techniques as the one implemented in our Institution is presented.

Methods: In our Institution, neuroendocrine tumor treatment, by radiopeptide infusion via intrahepatic arterial catheterization, is a well established technique. Kidney protective agents are also included in our protocol. The individualized patient dosimetry calculations were based on planar and SPECT scintigraphy images. Counts were determined in a region of interest (ROI) around the tumor, liver, kidneys and spleen. In planar technique, the ROIs were drawn in both anterior and posterior images while in SPECT counts measured per slice. For counts conversion to activities, calibration factors were calculated. Planar and SPECT images of cylindrical water - filled phantom, with five different known amounts of activity, were obtained. Corrections for scatter attenuation, collimator efficiency and detector response were calculated. In bone marrow dosimetry, blood based methods were used as in ^{177}Lu images no significant counts at bone or red plasma activity are displayed. Absorbed doses were calculated using MIRD formalism and S values were calculated using the RADAR system.

Results: The absorbed doses to organ per unity administered activity were comparable for both planar and SPECT techniques. On average, the absorbed dose was in tumor [4-40]mGy/MBq, in kidneys[0.25-1.05]mGy/MBq, in the bone marrow[0.01-0.13]mGy/MBq, in the spleen [0.3-2.1]mGy/MBq and in the liver [0.05-0.34]mGy/MBq.

Conclusion: In order to deliver higher dose to tumor and avoid kidneys and red marrow toxicity, accurate individualized dosimetry is obligatory. Furthermore, the results quantitatively confirm the therapeutic efficacy of transhepatic administration and introduce ^{177}Lu labeled peptide as an ideal for peptide receptor radiotherapy

Oral presentation

Consolidation Anti-CD22 Fractionated Radioimmunotherapy (RIT) with 90Y-Epratuzumab Tetraxetan Following R-CHOP in Elderly Diffuse Large B-cell Lymphoma (DLBCL) Patients

PALLARDY AMANDINE¹, BODET-MILIN CAROLINE¹, SOUBEYRAN PIERRE², GARIN ETIENNE³, COUTURIER OLIVIER⁴, ROUSSEAU CAROLINE¹, VUILLEZ JEAN-PHILIPPE⁵, SALAUN PIERRE-YVES⁶, CAMPION LOIC¹, WEGENER WILLIAM A⁷, GOLDENBERG DAVID M⁸, BARBET JACQUES¹, FAIVRE-CHAUVET ALAIN¹, KRAEBER-BODERE FRANÇOISE¹

¹ CHU/ICO/Inserm U892, Nantes, France

² Bergonié Institut, Bordeaux, France

³ Eugène Marquis Cancer Center, Rennes, France

⁴ CHU, Angers, France

⁵ CHU, Grenoble, France

⁶ CHU, Brest, France

⁷ Immunomedics, Morris Plain, NJ, USA

⁸ Garden State Cancer Center, Center for Molecular Medicine and Immunology, Morris Plains, NJ, USA
francoise.bodere@chu-nantes.fr

Objectives: A French phase II trial sponsored by the LYSA group assessed fractionated 90Y-epratuzumab tetraxetan as consolidation after front-line R-CHOP in untreated elderly (age >60 yrs) patients with stage I/II bulky or III/IV DLBCL.

Methods: Treatment included 6 cycles of R-CHOP14 followed 8 wks later by 2 infusions of 90Y-epratuzumab tetraxetan (15 mCi/m² [555 MBq/m²]), 7 days apart.

Results: 75 patients have been accrued prospectively and 61 (81.2%) received RIT. RIT toxicity consisted of grade 3-4 neutropenia in 46/61 patients (75.4%), anemia in 15 (24.6%), and thrombocytopenia in 47 (77.0%). Two patients developed myelodysplastic syndrome. Based on the 1999 International Workshop for Response Criteria, overall response rate (ORR) after 6 R-CHOP14 was 94.6% (71/75), with complete/unconfirmed complete responses (CR/CRu) in 52 patients (69.3%) and partial responses (PR) in 19 patients (25.3%). In an intention-to-treat analysis, CR/CRu rate after RIT was 72.0% (N=54), 7 patients (9.3%) remained in PR, and 8 (10.7%) progressed. At a median follow-up of 37.0 mos (1 to 55), the estimated 2-year progression-free-survival (PFS) was 72.4 % (60.6-81.2%) and overall survival (OS) 82.6% (71.4-89.8%). For the 61 patients treated by RIT, ORR was 91.8% (56/61), with 81.9% (50/61) CR/CRu; 8/16 patients (50.0%) converting to CR/CRu after RIT; the estimated 2-year PFS was 78.3% (65.6 - 86.8%), and OS 87.6 % (75.8 - 93.9%).

Conclusion: Fractionated 90Y-epratuzumab tetraxetan as consolidation after R-CHOP is tolerable in elderly untreated patients. PFS compares favorably to R-CHOP alone.

Poster

Production and characterization of monoclonal antibodies specific for dog and cat syndecan-1 for nuclear medicine preclinical trial on spontaneous tumors

DIAB M.¹, DAVODEAU F.¹, CHEREL M.^{1,2}

¹ Nantes-Angers Cancer Research Center CRCNA/ INSERM UMR892, Nantes, France.

² ICO cancer center, Nantes, France

maya.diab@univ-nantes.fr

BACKGROUND: Syndecan-1 (CD138) is a cell surface heparane sulfate bearing proteoglycane, over expressed in multiple myeloma and in a wide spectrum of carcinomas.

Syndecan-1 plays a crucial role in tumorigenesis therefore is an attractive target for cancer imaging and therapy. The objective of this study was to produce a monoclonal antibodies targeting canine CD138 in order to evaluate their usefulness for imaging and radioimmunotherapy on dogs with spontaneous carcinoma.

METHOD: Hybridomas were produced through immunization of mice with the recombinant ectodomain of canine syndecan 1 (residues 1 to 251) and fusion of spleen cells with Sp2/o cells. Screening of positive hybridomas by FACS was performed using canine CD138 transfected CHO cells. Isotypes and affinity were determined and Monoclonal antibodies were characterized using immunohistochemistry.

RESULTS: We selected twenty four hybridomas producing antibodies reacting with our CD138c transfected CHO cells. Only eleven hybridomas were isolated after subcloning allowing us to produce eleven different antibodies. All of them are IgG1 kappa except one which is IgG2b kappa. KD calculation showed a high affinity of these antibodies against canine CD138 antigen. Immunohistochemistry analysis showed that all antibodies recognize canine syndecan on normal and tumor tissues. Some antibodies recognize also the feline antigen.

CONCLUSION: These monoclonal antibodies could be a powerful tool to assess canine syndecan-1 targeting by imaging and radioimmunotherapy in clinically relevant large animal model.

SESSION 2 : Functional and phenotype imaging

Oral presentation

Regional analysis of ^{18}F -FDG and ^{18}F -Florbetapir PET in elderly, mild cognitive impairment and Alzheimer's disease

M Bailly¹, MJ Santiago Ribeiro^{1,2,4}, J Vercouillie^{1,2}, C Hommet³, V Camus³, D Guilloteau^{2,4}

¹ Nuclear Medicine Department, CHRU Hôpitaux de Tours, Tours, France

² Inserm U930, Université François Rabelais, Tours, France

³ Memory Clinic, CMRR, CHRU Hôpitaux de Tours, Tours, France

⁴ CIC-IT 806, Tours, France

matthieu.bailly@orange.fr

Objectives: To compare regional cerebral metabolic rate of glucose metabolism and amyloid-beta density in patients with Alzheimer's disease (AD), mild cognitive impairment (MCI) and healthy elderly subjects.

Methods: 18 patients (6 AD, 5 amnesic MCI and 7 controls) were enrolled at University Hospital of Tours, France, and submitted to clinical, neuropsychological and magnetic resonance imaging exams. PET images using ^{18}F -Florbetapir (mean activity injected: 266MBq) and ^{18}F -FDG (mean activity injected: 185MBq) were acquired. Standard uptake value ratio (SUVr) between cortical specific regions and cerebellum (used as non-specific activity) were defined using PMOD 3.2 software.

Results: The mean values of ^{18}F -FDG SUVr were significantly lower in frontal, anterior cingulate and temporal regions in MCI patients than in normal elderly (-15%, -22% and -11% respectively). AD patients showed global cerebral metabolic rate of glucose metabolism decrease, especially in parietal and precuneus regions (-15% and -13% compared to healthy control subjects). Precuneus and parietal cortex seem to be the most discriminative regions between AD and MCI patients. Only precuneus cortex showed an increased ^{18}F -Florbetapir uptake in AD. Combined the use of these two modalities (cerebral metabolic rate of glucose metabolism and amyloid-beta density) improves diagnostic accuracy for MCI and AD.

Conclusion: In this study, ^{18}F -FDG shows to be superior to ^{18}F -Florbetapir to distinguish normal elderly, MCI and AD. These results suggest that ^{18}F -FDG PET remains a major candidate modality for detecting brain metabolic changes in MCI and AD, in the growing development of amyloid PET radiotracers.

This work has been supported in part by a grant from the French National Agency for Research called "Investissements d'Avenir" n°ANR-11-LABX-0018-01.

SESSION 2 : Functional and phenotype imaging

Oral presentation

In vivo PET quantification of the dopamine transporter in rat brain with [^{18}F]LBT-999 and application in a rat model of Parkinson's disease

Sophie Sérrière^{1,2}, Clovis Tauber^{1,2}, Johnny Vercouillie^{1,2}, Denis Guilloteau^{1,2,3}, Jean-Bernard Deloye⁴, Lucette Garreau^{1,2}, Laurent Galineau^{1,2}, **Sylvie Chalon**^{1,2}

¹*Inserm, U930, Tours, France*

²*Université François-Rabelais de Tours, UMR-U930, Tours, France*

³*CHRU de Tours, Hôpital Bretonneau, Service de Médecine Nucléaire in vitro, Tours, France*

⁴*Laboratoires Cyclopharma, Tours, France*

sylvie.chalon@univ-tours.fr

Objectives: We examined whether [^{18}F]LBT-999 ((*E*)-*N*-(4-fluorobut-2-enyl)2 β -carbomethoxy-3 β -(4'-tolyl)nortropane) is an efficient positron emission tomography (PET) tracer for the quantification of the dopamine transporter (DAT) in the healthy and 6-hydroxydopamine-lesioned rat brain.

Methods: PET studies were performed in healthy male Wistar rats using several experimental designs, i.e. test-retest, co-injection with different doses of unlabelled LBT, displacement with GBR12909 and pre-injection of amphetamine. In a second step, we used [^{18}F]LBT-999 for the follow-up of the DAT density in a rat model of Parkinson's disease obtained by an unilateral striatal injection of 6-hydroxydopamine (6-OHDA).

Results: The brain uptake of [^{18}F]LBT-999 confirmed its specific binding to the DAT. The non-displaceable uptake (BP_{ND}) in the striatum, between 5.37 and 4.39, was highly reproducible and reliable, and was decreased by 90% by acute injection of the DAT inhibitor GBR12909. In the substantia nigra/ventral tegmental area (SN/VTA), the variability was higher and the reliability was lower. Pre-injection of the dopamine releaser amphetamine induced decrease of [^{18}F]LBT-999 BP_{ND} of 50% in the striatum.

In 6-OHDA-lesioned rats, the accumulation of [^{18}F]LBT-999 was significantly decreased (40-50%) in the ipsilateral striatum as early as 24 h post-lesion; this decrease reached around 70-80% in same animals, at 3 days post-lesion.

Conclusions: [^{18}F]LBT-999 allows the quantification of the DAT by PET in living rat brain with high reproducibility, sensitivity and specificity. This tracer is also useful for studying the progressive dopaminergic neuron degeneration after lesion. Thus it will be a relevant tool for the follow-up of potential treatments in preclinical models of brain disorders involving the DAT.

Oral presentation

Relationship between clinical features of Lewy pathology and dopaminergic function throughout the Alzheimer Disease Dementia with Lewy bodies spectrum.

Amandine Pallardy¹, Sarah Evain², Thibaud Lebouvier², Thomas Carlier¹, Martine Vercelletto², Pascal Derkinderen², Françoise Kraeber-Bodéré¹, Claire Boutoleau-Bretonnière².

¹ Service de médecine nucléaire, CHU de Nantes, boulevard Jacques-Monod, 44093 Nantes Cedex.

² Centre Mémoire Recherche et Ressources (CMRR), Neurologie, Hôpital Laënnec, CHU de Nantes, boulevard Jacques-Monod, 44093 Nantes Cedex.

amandine.pallardy@chu-nantes.fr

Hypothesis: Current diagnostic criteria do not take into account the huge clinical and histopathologic overlap between Dementia with Lewy bodies (DLB) and Alzheimer disease (AD). Indeed, AD pathology is nearly constant in DLB and up to 40% of AD patients present with Lewy pathology (Lebouvier et al., Rev Neurol. 2013). To better explore this continuum, we postulated that alterations of the substantia nigra, relatively specific to Lewy pathology in the context of an incipient dementia, were a good estimate of the Lewy pathology burden in the whole brain.

Methods: We confronted a selection of 8 clinical features of Lewy pathology (parkinsonism, hallucinations, fluctuations, cardiovascular dysautonomia, vesical and sphincter dysfunction, REM behavior disorders, olfactory dysfunction and cognitive decline) to [18F]fluorodopa Positron Emission Tomography (PET) in patients with a cognitive decline attributed to AD or DLB. PET data were assessed by volume-of-interest analysis using the software PMOD-Dopasoft. Specific uptake region-to-occipital ratios (SUR) were determined for striatum (STR), putamen (PUT), and caudate nucleus (CAU).

Results: Nine patients were studied; 3 fulfilled diagnostic criteria for probable AD, 3 for probable DLB, 3 for possible AD and/or possible DLB. All had between 5 to 8 pathological features of Lewy pathology.

There was no difference between left and right SUR for STR, PUT or CAU. The mean SUR for PUT and STR correlated significantly with the number of pathological features of Lewy pathology ($p < 0.01$ and 0.02 respectively). There was no significant correlation between Mini Mental State Examination or disease duration and PUT or STR SUR.

Conclusion: A dual clinical and functional approaches may allow diagnosis of Lewy body pathology as a dominant as well as a concomitant disease. Although these preliminary results need to be confirmed, they pave the way to a refinement of the diagnostic criteria, allowing identification of the Lewy body variant of AD.

Oral presentation

Early changes in brain metabolism following vagal stimulation

Charles-Henri Malbert¹, Sylvie Guérin¹, Eric Bobillier¹, Alain Chauvin², Francis Legouevéc², Jean-Louis Divoux³

¹ ADNC unit, INRA, 35590 Saint-Gilles, France

² PEGASE unit, INRA 35590 Saint-Gilles, France

³ Obelia/Groupe MXM, 2720, route de St Bernard, F-06224 VALLAURIS France
Charles-Henri.Malbert@rennes.inra.fr

Hypothesis: Vagal stimulation is an effective neurophysiological treatment for patients with refractory epilepsy. It is also effective for depression and we recently demonstrated its potential to reduce food intake. However, the mechanism of action remains unclear. There are differences in brain structures activated mainly depending of the duration of the stimulation; acute or several weeks. The aim of our study as to evaluate the changes in brain metabolism obtained by FDG PET scanning 7 days after the onset of vagal stimulation on a porcine model.

Methods: 6 growing pigs (31 ± 4.5 Kg) were fitted with two set of silicone vagal cuff comprising each two platinum electrodes using a laparoscopic approach of the abdominal vagi. 6 additional animals were sham operated without the placement of silicone cuff around the vagi. Stimulation was started the following day and continued until the PET imaging session. Stimulation parameters were identical those formerly used by our group: 2 mA amplitude, Frequency of pulse train 30 Hz for 500 µs pulses. The duration of the train was 30 s and the interval between trains was 5 minutes.

For PET scanning, the animals were anesthetized using isoflurane and artificially ventilated. Fluorodexoxyglucose (¹⁸FDG – 250 MBq) was injected in the marginal ear vein. Images were acquired 45 minutes after injection using a HR+ PET scanner in 3D mode and corrected using transmission scan using rotating ⁶⁸Ge rods. The data were analyzed with statistical parametric mapping (SPM 8) with an in-house build PET template co-registered with a porcine numerical atlas.

Results: Four areas were activated by vagal stimulation compared to sham animals (p<0.0001 with FDR): cingular cortex, putamen, caudate nucleus and substantia nigra/tegmental ventral area. All these areas participate to the reward network. Despite lowering the analysis threshold (p<0.01) we were not able to observe an altered metabolism of the dorsal vagal complex or the thalamus.

Conclusion: Vagal stimulation activates almost all the areas included in the reward network with the exception of the orbitofrontal cortex. This activation explains several of the behavioral effects obtained by chronic vagal stimulation.

SESSION 2 : Functional and phenotype imaging

Oral presentation

Relationship between β -amyloid density and cortical perfusion in Posterior Cortical Atrophy and Progressive Primary Aphasia

MJ Santiago-Ribeiro^{1,2,3}, E Beaufile⁴, J Vercouillie², K Mondon^{2,4}, V Camus^{2,4}, D Guilloteau^{1,2,3}, C Hommet^{2,4}

¹ Nuclear Medicine Department, CHRU, Tours, France

² Inserm U930, Université François Rabelais, Tours, France

³ CIC-IT 806, Tours, France

⁴ Memory Clinic, CMRR, CHRU, Tours, France

maria.ribeiro@univ-tours.fr

Objectives: Posterior cortical atrophy (PCA) and progressive primary aphasia (PPA) are characterised by hypoperfusion predominating in parieto-occipital and temporal cortex for PCA and PPA respectively. In this study we evaluated the relationship between cortical perfusion and cerebral β -amyloid density in PCA and PPA.

Methods: Eight PCA patients and 8 PPA patients were submitted to a SPECT study (Symbia γ -camera, Siemens) 30 min after a mean injected dose of 835 MBq of ^{99m}Tc-ECD or ^{99m}Tc-HMPAO. All the subjects were submitted to a 10 min PET acquisition, 50 min after injection of ¹⁸F-AV45 (208 MBq) (Gemini Dual tomography, Philips). Regions of interest were defined for frontal, posterior cingulate, precuneus, parietal, temporal and occipital cortex and for cerebellum (the reference region used to obtain SUVR) for ¹⁸F-AV45 images using Syngo.via (Siemens). For SPECT studies we used Scenium (Siemens) to compare perfusion on left and right parietal, temporal and occipital cortex to a database of normal controls.

Results: In PCA group a severe hypoperfusion was observed in parietal-occipital region. In PPA group hypoperfusion was found in left temporal cortex for 5 patients and temporal bilaterally for three. In PCA SUVRs (mean \pm SD) were 1.23 \pm 0.21, 1.27 \pm 0.21, 1.18 \pm 0.18, 1.14 \pm 0.19, 1.20 \pm 0.15 and 1.20 \pm 0.15 for frontal, posterior cingulate, precuneus, parietal, temporal and occipital cortex, respectively. For PPA, SUVR were lower but not significant different and were, for the same ROI, 1.07 \pm 0.24, 1.20 \pm 0.20, 1.06 \pm 0.28, 1.05 \pm 0.23, 1.05 \pm 0.24 and 1.11 \pm 0.21.

Conclusion: No cortical significant differences in ¹⁸F-AV45 binding between PCA and PPA were founded whereas cortical focal perfusion patterns were distinct in PCA and PPA. These results suggest that PCA and PPA syndromes are associated with degeneration of functional networks that are not explained by the distribution β -amyloid deposition.

This work has been supported by grants from French National Agency for Research ("Investissements d'Avenir" ANR-11-LABX-0018-01), FEDER and the *Fondation Thérèse Planiol*.

Oral presentation

Brain kinetics of ^{18}F -DPA-714 in acute and chronic neuroinflammation

MJ Santiago-Ribeiro^{1,2,3}, J Vercouillie², N Arlicot², B Erra^{1,2}, S Maia¹, P Corcia^{2,4}, I Bonnaud⁴, S Debiais⁴, M Kassiou⁵, D Guilloteau^{1,2,3}

¹ Nuclear Medicine Department, CHRU, Tours, France

² Inserm U930, Université François Rabelais, Tours, France

³ CIC-IT 806, Tours, France

⁴ Neurology Medicine Department, CHRU, Tours, France

⁵ School of Chemistry, University Sydney, BMRI, Medical Radiation Sciences, Sydney, NSW, Australia
maria.ribeiro@univ-tours.fr

Objectives: The translocator protein 18kDa (TSPO), although minimally expressed in healthy brain, is upregulated in pathological conditions, coinciding with microglial activation. It is thereby a suitable *in vivo* biomarker of neuroinflammation for detection, evaluation and therapeutic monitoring of brain diseases. We aimed to evaluate in healthy controls (HC) and in two different pathological situations the cerebral kinetics of the PET TSPO radioligand ^{18}F -DPA-714.

Methods : 14 subjects (6 HC; 4 recent stroke patients; 4 patients with amyotrophic lateral sclerosis, ALS) were submitted to a PET study for 90 min after the injection of ^{18}F -DPA-714 (mean injected activity: 260 MBq). Time activity curves (TAC) were obtained for several cortical regions but also for striatum, thalamus and cerebellum using volumes of interest (VOI) defined with Pmod software and using MNI-AAL atlas.

Results: For all subjects, brain maximal uptake of ^{18}F -DPA-714 is observed 5 min pi. For HC, this phase is followed by two periods of decay: a fast phase between 5 and 30 min pi, followed by a slower phase until the end of the acquisition. In patients with ALS, two washout phases were also observed but the first is observed between 5 and 45 min pi. Finally, in the case of patients presenting an acute stroke, the rapid washout phase occurs between 5 and 15 min pi.

Conclusion: Our results show a peak of similar ^{18}F -DPA-714 brain uptake for all subjects, followed by two stages of decay, a fast and a slow, however different appearance depending on the type of pathology, acute or chronic. This PET radiotracer will be very useful for the exploration of neurodegenerative diseases or acute pathological profiles as also for therapeutic monitoring.

This work has been supported by grants from French National Agency for Research (Investissements d'Avenir ANR-11-LABX-0018-01) and FP7-HEALTH-2011 (INMiND-Imaging of Neuroinflammation in Neurodegenerative Diseases)

Oral presentation

3'-FLUORINE-18-3'-DEOXY-L-THYMIDINE (FLT) POSITRON EMISSION TOMOGRAPHY (PET): AN ACCURATE AND EFFECTIVE TOOL FOR ASSESSING TUMOR RESPONSE IN BREAST CANCER

Olivier Couturier¹, Caroline Rousseau², Jean-Yves Pierga³, Alina Berriolo-Riedinger⁴, Jean-Louis Alberini⁵, Sylvie Girault⁶, Pierre Fumoleau⁴, Etienne Brain⁵, Sophie Abadie-Lacourtoisie⁶, Pierre Vera⁷, Jean-Claude Liehn⁸, Pierre Olivier⁹, Lionel Uwer¹⁰, Florent Cachin¹¹; Christine Sagan¹²; Francis Bouchet¹, Nicolas Lebas⁵; Christel Mesleard¹³; Emmanuelle Fourme⁵; Anne-Laure Martin¹³, Pierre Lovinfosse¹, Franck Lacœuille¹, Mario Campone²

1 Centre Hospitalier Universitaire, Angers, France; 2 Institut de Cancérologie de l'Ouest, Saint Herblain, France; 3 Institut Curie, Paris, France; 4 Centre Georges-François Leclerc, Dijon; 5 Institut Curie, Saint-Cloud, France; 6 Institut de Cancérologie de l'Ouest, Angers, France; 7 Centre Henri Becquerel, Rouen, France; 8 Institut Jean Godinot, Reims, France; 9 Centre Hospitalier Universitaire, Nancy, France; 10 Institut de Cancérologie de Lorraine, Vandoeuvre les Nancy, France; 11 Centre Jean Perrin, Clermont Ferrand, France; 12 Centre Hospitalier Universitaire, Saint-Herblain, France; 13 R&D UNICANCER, Paris, France
ocouturier70@me.com

Objectives: A French multicenter study was promoted by the national French cancer federation (Unicancer R&D) to assess the potential of [¹⁸F]FLT (positron emission tomography (PET) biomarker of proliferation) to manage breast cancer neoadjuvant chemotherapy (NAC). The main objective was to compare changes in tumor [¹⁸F]FLT uptake to histopathological changes induced by NAC, assuming an arrest of tumor growth related to the effectiveness of NAC.

Methods: 97 patients (age 48.6 +/- 10.2 y.) were included in 13 nuclear medicine centers. All patients were eligible to anthracycline-based NAC for a *de novo* unifocal breast cancer (ductal n=84, lobular=11, other type= 2; stage II n=75, stage III n=21 et stage IV n=1). 90 patients underwent a baseline PET before the onset of NAC (PET1) and a final PET after the end of NAC and before surgery (PET3). PET acquisitions were performed 60±7min after FLT injection. SUVmax (maximum standardized uptake value), SUVpeak (1 cm³ ROI including pixel max) and SUV41 (isocontour 41% of pixel max) were computed. Changes in SUV on PET3 vs PET1 were analyzed in relation to histopathological findings at the end of NAC (Sataloff criteria).

Results: Tumor FLT uptake decreased markedly between TEP1 and TEP3 (SUVmax = 6.2±4.8 vs 1.3±1.2 respectively; SUVpeak= 4.6±3.2 vs 0.9±0.9; SUV41=3.6±2.8 vs 0.8±0.7). Total or near-total therapeutic effect (grade A) were obtained in 20 patients, more than 50% therapeutic effect but less than total or near-total effect (grade B) in 37 patients, less than 50% therapeutic effect but visible effect (grade C) in 22 patients, or no therapeutic effect (grade D) in 11 patients. SUVmax decreased dramatically (87.5%) to background levels in all patients with a complete response (grade A). Overall, changes in SUV differed depending on the type of histological response (p<0.01) i.e. SUVmax changes were more pronounced as pathological responses were good: 61% for grade D; 65.7% grade C and 69.8% grade B. The same results were obtained with the two other SUV types.

Conclusions: Pathologic response to NAC in breast cancer can be assessed accurately by FLT.

SESSION 2 : Functional and phenotype imaging

Oral presentation

Assessment of hypoxia with 3-[¹⁸F]-fluoro-1-(2-nitro-1-imidazolyl)-2-propanol ([¹⁸F]-FMISO): a noninvasive tool to improve treatment efficacy in GBM

Corroyer-Dulmont Aurélien^{1,2,3,4}, Pérès Elodie A.^{1,2,3,4}, Petit Edwige^{1,2,3,4}, Durand Lucile^{1,2,3,4}, Toutain Jérôme^{1,2,3,4}, Divoux Didier^{1,2,3,4}, Roussel Simon^{1,2,3,4}, MacKenzie Eric T.^{1,2,3,4}, Barré Louisa^{1,2,3,4}, Bernaudin Myriam^{1,2,3,4} and Valable Samuel^{1,2,3,4}.

¹CNRS, UMR ISTCT 6301, CERVOxy and LDM-TEP Groups. GIP CYCERON, Bld Henri Becquerel, BP 5229, 14074 CAEN cedex, France

²University of Caen Basse-Normandie, UMR ISTCT 6301, CERVOxy and LDM-TEP Groups

³CEA, DSV/I2BM, UMR ISTCT 6301, CERVOxy and LDM-TEP Groups

⁴Normandie Univ

corroyer@cyceron.fr

Despite multiple advances in cancer therapies, patients with glioblastoma (GBM) still have a poor prognosis. Numerous glioma models are used not only for the development of innovative therapies but also to optimize conventional treatments. Given the significance of hypoxia in drug and radiation resistance and that hypoxia is widely observed in GBM, the establishment of reliable methods to map hypoxia in preclinical models may contribute to the discovery and translation of more targeted therapies as well as to optimization of radio/chemotherapy. The aim of this study was to analyse through FMISO PET imaging the hypoxic status of two commonly used rat (9L and C6) and human (U87 and U251) orthotopic glioma models developed in rats. In parallel, because of the relationships between angiogenesis and hypoxia, we used Magnetic Resonance Imaging (MRI), immunohistochemistry to characterize the tumoral vasculature. Although all tumors were detectable in T2-weighted MRI and 2-deoxy-2-[¹⁸F]-fluoro-d-glucose-μPET [¹⁸F]-FDG, only the U251 and the C6 models exhibited [¹⁸F]-FMISO uptake. In line with these results, U251 and C6 tumors were less densely vascularized than U87 and 9L tumors as assessed by MRI and vascular immunohistochemistry. Our study demonstrates the benefits of noninvasive imaging of hypoxia and characterization of tumor vascularization in preclinical models to define the most reliable for translation of future therapies to the clinic based on the importance of intratumoral oxygen tension for the efficacy of radio/chemotherapy.

We thank the European Regional Development Fund of Basse-Normandie (FEDER), the Conseil Régional de Basse-Normandie and the French National Agency for Research called "Investissements d'Avenir" n°ANR-11LABX0018-01.

SESSION 2 : Functional and phenotype imaging

Oral presentation

⁶⁸Ga-DOTANOC PET/CT IN WELL-DIFFERENTIATED GASTRO-ENTEROPANCREATIC NEUROENDOCRINE TUMORS (GEP-TNEs): PROSPECTIVE COMPARISON WITH SOMATOSTIN RECEPTOR SPECT/CT AND FOUR-PHASE CT: PRELIMINARY RESULTS

C. Mathieu¹, M.Colombie², T.Matysiak³, B.Dupas⁴, V.Rohmer⁵, O. Couturier⁶, O. Morel⁷, E.Mirallie⁸, D.Druil⁹, A.Faivre-Chauvet¹⁻¹⁰, F.Kraeber-Bodéré¹⁻²⁻¹⁰, C. Ansquer¹⁻¹⁰

1 Nuclear Medicine Unit, University Hospital, Nantes, FRANCE

2 Nuclear Medicine Unit, ICO Cancer Center, St Herblain, FRANCE

3 Gastroenterology Unit, University Hospital, Nantes, FRANCE

4 Radiology Unit, University Hospital, Nantes, FRANCE

5 Endocrinology Unit, University Hospital, Angers, FRANCE

6 Nuclear Medicine Unit, University Hospital, Angers, FRANCE

7 Nuclear Medicine Unit, ICO Cancer Center, Angers, FRANCE

8 Endocrine surgery Unit, University Hospital, Nantes, FRANCE

9 Endocrinology Unit, University Hospital, Nantes, FRANCE

10 CRCNA INSERM U892, Nantes, FRANCE

cedric.mathieu44@gmail.com

Objectives: Well-differentiated GEP-TNEs are explored in clinical practice using OctreoScan and CT. The aim of this prospective study was to compare the diagnostic value of ⁶⁸Ga-DOTANOC PET/CT to conventional imaging in patients with proven or suspected GEP-TNE.

Materials and methods: 22 patients (13M, 9F) underwent whole body four-phase CT, whole body OctreoScan SPECT/CT and ⁶⁸Ga-DOTANOC PET/CT within two months for initial staging (n=13), suspicion of relapse (n=6) or detection of unknown primary tumor (n=3). Each imaging was interpreted blindly and separately. The gold standard (GS) was based on available histologic, imaging, and follow-up findings (>6 months). Sensitivity of each modality was assessed in a per-lesion analysis.

Results: A total of 106 lesions were detected by imaging, including 80 lesions confirmed by the GS. Moreover, histology concluded to 2 additional lesions not detected by imaging. Among the 82 confirmed lesions, 16 were in pancreas, 47 in liver, 13 in lymph nodes, 5 in duodenum or bowels and 1 in peritoneum. PET detected all of the lesions except the two lymph nodes found only by histology. OctreoScan didn't detect any additional lesion compared with CT or PET. Overall sensitivity of PET, OctreoScan and CT were 97%, 55%, and 88%, respectively. Sensitivity for liver was 100%, 62% and 96% for PET, OctreoScan and CT, respectively, for bowels 100%, 20% and 40%, for pancreas 100%, 44% and 81% and for lymph nodes 85%, 62% and 85%.

Conclusion: OctreoScan, even optimized by whole body SPECT/CT, is the less effective method for detection of GEP-NET lesions. ⁶⁸Ga-DOTANOC PET/CT shows a higher sensitivity as compared to Octreoscan and four-phase CT, allowing to better guide clinical management of patients.

Oral presentation

Development of Affitins for tumor targeting

Matous E.¹, Pecorari F.¹, Chérel M., and Mouratou B

¹ CRCNA, INSERM UMR 892 / CNRS 6299 / Université de Nantes Institut de Recherche Thérapeutique de l'Université de Nantes 8, quai Moncousu BP 70721 44007 NANTES Cedex 1
etienne.matous@univ-nantes.fr

Objective: We developed an alternative to antibodies for tumor targeting currently used in cancer imaging and therapy : Affitins. Monoclonal antibodies remain the best tool for antigenic targeting since 40 years. However, in the context of imaging, their use have limits mainly due to their physic and pharmacokinetic properties. This triggers poor diffusion to the tumor site and rapid clearance [1]. In that way, several alternatives were developed to decrease the size of vectors, for exemple Diabodies, Nanobodies, Ankyrin, and Affitins [2]. We developed here the generation of Affitin directed against a family member of syndecan : CD138 or syndecan I [3].

Experimental methods used: A selection by ribosome display against CD138 was performed, and a screening of the selection pool by flow cytometry allowed us to isolate several Affitins with specific binding to CD138. *In vivo* studies were performed in a murine model of multiple myeloma induced by injection of 10 millions of MDN human multiple myeloma cells in ScidB mice. Biodistribution studies were performed with both ¹²⁵I radiolabeled Affitin and immunohistochemistry.

Results: Best affinity was mesured for A872 with 40 nM and *in vitro* studies showed a specific binding to several cell lines, a high thermal and chemical stability, and a resistance to blood proteases. Concerning *in vivo* studies, a biodistribution in mice showed that this scaffold posseses a pharmacokinetic well adapted to phenotype imaging and we showed by using immunohistochemistry that A872 Affitin is also able to bind specifically to CD138 overexpressing tumor.

Conclusion: We present here the development of a new tool for CD138 targeting. A872 Affitin showed a high and specific binding to this target. Moreover, this Affitin displayed a specific tumor targeting in our murine model of multiple myeloma, and therefore is a good candidate to perform phenotype imaging.

1. Chames, P., et al., *Therapeutic antibodies: successes, limitations and hopes for the future*. British journal of pharmacology, 2009. **157**(2): p. 220-33.
2. Mouratou, B., et al., *Remodeling a DNA-binding protein as a specific in vivo inhibitor of bacterial secretin PulD*. Proc Natl Acad Sci U S A, 2007. **104**(46): p. 17983-8.
3. Wijdenes, J., et al., *A plasmocyte selective monoclonal antibody (B-B4) recognizes syndecan-1*. Br J Haematol, 1996. **94**(2): p. 318-23.

SESSION 2 : Functional and phenotype imaging

Oral presentation

A quantitative evaluation of the influence of Rituximab therapy and tumor growth on 2-[¹⁸F]Fludarabine uptake by PET/CT imaging in a follicular lymphoma xenograft model

Narinée Hovhannisyan, Stéphane Guillouet, Martine Dhilly, Fabien Fillsoye, Delphine Patin, Michel Leporrier, Louisa Barré

CEA, DSV/I2BM, LDM-TEP Group, GIP Cyceron, Bd Henri Becquerel, BP 5229, 14074 Caen Cedex, France

Université de Caen Basse-Normandie, Caen, France

CNRS, UMR ISTCT 6301, LDM-TEP Group, GIP Cyceron, Caen, France

hovhannisyan@cyceron.fr

Objectives: 2-[¹⁸F]Fludarabine is a novel Positron Emission Tomography (PET) radiotracer for imaging lymphoma. Our purpose was to evaluate the longitudinal changes of 2-[¹⁸F]Fludarabine in response to Rituximab therapy and tumor growth in a follicular lymphoma xenograft model.

Methods: CB17 SCID mice bearing human follicular DOHH-2 lymphoma were treated with Rituximab (10mg/kg) or physiological saline (vehicle) by intraperitoneal injection weekly for three weeks. 2-[¹⁸F]Fludarabine was injected (~15MBq) *via* tail vein and animals were imaged within 40-60 min after injection. PET/CT scans were performed a day before dosing for baseline imaging, and then approximately two and three weeks after onset of treatment. Growth of tumors was directly measured three times weekly based on an electronic external caliper for real-time evaluation of Rituximab or vehicle treatment response. Statistical evaluation of tumor growth was assessed by CT measurements. For tumor with necrotic core, the uptake analysis was realized with both entire tumor and metabolically active volume of tumor (MAVT) based segmentations.

Results: Rituximab treatment resulted in suppression of tumor growth ($p < 0.001$). No significant difference was observed in tumor volume changes for Rituximab-treated group during the follow-up ($p = 0.43$). The 2-[¹⁸F]Fludarabine uptake (%ID/cc) also remained constant throughout the experiment ($p = 0.93$). In contrast, the tumor volume continued to increase for vehicle-treated group; however, no significant correlation was observed between the tumor volume and the uptake value with either entire tumor ($r = 0.53$, $p = 0.05$) or MAVT analysis ($r = 0.36$, $p = 0.2$).

Conclusion: Rituximab treatment did not modulate 2-[¹⁸F]Fludarabine uptake in follicular DOHH-2 lymphoma model. Thus, 2-[¹⁸F]Fludarabine PET may be a promising method for Rituximab therapy monitoring in follicular lymphoma when, moreover, no influence of tumor size was observed on uptake level.

Oral presentation

Feasibility of pretargeted immuno-PET using an anti-CEA bispecific antibody and a ^{68}Ga -labeled hapten-peptide in metastatic breast and medullary thyroid carcinoma patients: preliminary results

C. Rousseau^{1,2}, A. Faivre-Chauvet^{2,3}, A. Rauscher^{1,2}, P. Baumgartner¹, T. Carlier^{2,3}, L. Ferrer^{2,4}, C. Bodet-Milin^{2,3}, D. Goldenberg^{5,6}, R Sharkey⁵, J. Barbet^{2,7}, F. Kraeber-Bodéré^{1,2,3}

¹Nuclear Medicine, ICO Cancer Center, Saint-Herblain

²CRCNA INSERM U892, Nantes,

³Nuclear Medicine, University Hospital, Nantes

⁴Physics Unit, ICO Cancer Center, Saint-Herblain

⁵Garden State Cancer Center, Center for Molecular Medicine and Immunology, Morris Plains, NJ, USA

⁶IBC Pharmaceuticals, Inc., and Immunomedics, Inc., Morris Plains, NJ, USA

⁷Arronax, Saint-Herblain, France

Immuno-PET is a non-invasive imaging technology based on detection and quantification of radiolabeled monoclonal antibodies, antibody fragments and pretargeted peptides. Two feasibility clinical studies are on going to optimize molar doses and pre-targeting delay of immuno-PET using the anti-CEA x anti-HSG humanized trivalent TF2 bispecific monoclonal antibody and the ^{68}Ga -IMP288 radio-labeled HSG peptide, in relapsing medullary thyroid carcinoma (MTC) or breast cancer (BC) patients. A similar design was originally intended for the 2 studies. Four cohorts of 3 patients receive different molar doses of TF2 and ^{68}Ga -IMP288 with variable pretargeting delay. For the first cohort of MTC and breast cancer patients, the antibody and peptide doses and the delay have been determined using pre-clinical animal data. For the other cohorts, the molar doses of TF2 and ^{68}Ga -IMP288 and the delay depend on the tumor uptake and background activity observed in the previous cohort. Patients underwent two PET scans 1 and 2 hours after ^{68}Ga -IMP288 injection.

Six patients (2 cohorts) with CEA-positive metastatic BC and 9 patients (3 cohorts) with MTC have been included. In the first cohort, the patients received 148.8 MBq [139-235.5] of ^{68}Ga -IMP288 (6 nmol) 24h after an injection of 120 nmol of TF2. For the MTC study, the blood compartment activity was relatively high and stable between 1 and 2 hours after the peptide injection but the tumor lesions showed a good stable uptake. As the tumor uptake was good in the first cohort but the blood background too high, the delay was increased to 30 hours for the second cohort. An improvement of tumor uptake was observed. Moreover, the ratio tumor-to- blood was increased. The results observed in the second cohort conducted to increase the delay to 42h in the third cohort. This delay did not achieve a significant improvement of tumor uptake and tumor-to-background ratio. For the breast cancer study, the data from the first cohort led to the same attitude as adopted for the MTC namely an increase of delay to 30h. In addition, the tumor uptake and the blood background noise were higher and more variable than in the MTC study. Between the first and second cohort, only a minor change in the tumor uptake was observed, with a large variability between patients. The cohorts IV of MTC and III of breast cancer are on-going. For the two studies, the patients will receive the same molar dose of TF2 and a lower molar dose of peptide (3 nmol) labeled with ^{68}Ga at a higher specific activity.

SESSION 2 : Functional and phenotype imaging

Poster

EFFECTIVE TARGETING OF ENDOMETRIAL TISSUE BY 16α - $[^{18}\text{F}]$ FLUORO- 17β -ŒSTRADIOL ($[^{18}\text{F}]$ -FES): PRELIMINARY RESULTS IN THE DIAGNOSIS OF ENDOMETRIOSIS

Céline LEFEBVRE-LACOEUILLE^{2,3}, Franck LACOEUILLE^{1,3}, Pacôme FOSSE¹, Francis BOUCHET¹, Anne CROUE⁴, François HINDRE³, Philippe DESCAMPS², **Olivier-François COUTURIER^{1,3}**

¹ Service de médecine nucléaire, CHU Angers, 4 rue Larrey, 49933 ANGERS France

² Service de gynéco-obstétrique, CHU Angers, 4 rue Larrey, 49933 ANGERS France

³ INSERM U1066, IBS-CHU Angers, 4 rue Larrey, 49933 ANGERS Cedex 9 France

⁴ Service d'anatomie pathologique, 4 rue Larrey, 49933 ANGERS France
ocouturier70@me.com

Objectives: Positron Emission Tomography with 16α - $[^{18}\text{F}]$ fluoro- 17β -estradiol (PET- $[^{18}\text{F}]$ FES) is used to evaluate the *in-vivo* tissue density in estrogen receptor (ER). We report here the first results for the diagnosis of endometriosis.

Materials and methods: Four patients with clinical and morphological signs (\pm pelvic ultrasound MRI) consistent with endometriosis were enrolled in this National Grant PHRC ENDOTEP. They underwent a PET- $[^{18}\text{F}]$ FES scan before laparoscopy (macroscopic and histological analysis, immuno-histochemical ER expression).

Results: In the four patients, the diagnosis of endometriosis was confirmed on the typical macroscopic appearance of laparoscopy plus histological analysis of at least one lesion. No uptake of $[^{18}\text{F}]$ FES by endometriosis lesions were observed in the first three patients with continuous estrogen-progestin therapy. The fourth patient, untreated and in the first part of the menstrual cycle when performing PET- $[^{18}\text{F}]$ FES had however an increased $[^{18}\text{F}]$ FES uptake of one lesion of endometriosis confirmed by laparoscopy.

Conclusion: $[^{18}\text{F}]$ FES could lead to noninvasively diagnose endometriosis in patients not receiving hormonal treatment.

SESSION 2 : Functional and phenotype imaging

Poster *

Ani-Scans: an experimental nuclear imaging facility for large animal in Rennes

Nicolas Coquery^{1,2}, Gwénaëlle Randuineau^{1,2}, Sylvie Guérin^{1,2}, Paul Meurice^{1,2}, Isabelle Nogret^{1,2}, Eric Bobillier^{1,2}, David Val-Laillet^{1,2}, Charles-Henri Malbert¹

¹ PRISM, Ani-Scans, Saint Gilles, France

² INRA, UR1341 ADNC (Alimentation & Adaptations Digestives, Nerveuses et Comportementales), Saint Gilles, France

nicolas.coquery@inra.rennes.fr

PRISM ("Plateforme Rennaise d'Imagerie et de Spectroscopie Structurale et Métabolique") is a multicomponent facility (Rennes 1 University, IRSTEA and INRA) dedicated to multimodal imaging (RMN, IRM, CT, PET) from molecular structure to large animal. The component Ani-Scans (INRA, Saint Gilles) is devoted to nuclear imaging in the pig model (CT, PET, SPECT) in close relationship with the ADNC ("Alimentation et adaptations Digestives, Nerveuses et Comportementales") research department.

The pig, which shares many anatomical and physiological features with the human, has been increasingly used as a good alternative model to primates and rodents in biomedical research. Indeed, the size of the animal, the organs physiology, the capability of performing complex behavioural tasks makes the pig an ideal model for translational studies.

Some imaging protocols are already in routine use within Ani-Scans activity. Phenotypic characterization is usually performed with CT scan procedures with or without image-guided biopsies. Functional imaging of the proximal gut represents an historical feature of the platform and includes gastric emptying and motility measurements in conscious animals using dynamic gamma scintigraphy. Anatomical and functional imaging of the pig's brain has been developed within the last six years. It uses several modalities including PET, SPECT. The imaging processes range from the production of anatomical templates to functional and molecular imaging. Functional brain imaging relates to microvascularisation (^{99m}Tc-HMPAO), permeability of the brain-blood barrier (^{99m}Tc-DTPA) and glucose brain metabolism (¹⁸FDG). Molecular imaging strategies currently available include dopamine and sympathetic systems imaging but other neuropeptides and physiological features will be explored in the future.

Ani-Scans also profits from complementary resources: a radioprotected animal facility, and an experimental surgery facility. Besides its activities in methodological research and development, Ani-Scans provides services to the public and private sectors.

SESSION 2 : Functional and phenotype imaging

Poster *

AVIESAN Strategic Valorization Field on Imaging Agents

Sabin Carme¹, Denis Guilloteau², Franck Denat³

¹ AVIESAN Paris, France

² University of Tours, France

³ University of Burgundy, France

e-mail : sabin.carme@aviesan.fr

Objective: Created in April 2009, the French National Alliance for Life Sciences and Health (AVIESAN) groups together the main stakeholders of life and health sciences in France. Within AVIESAN, the Strategic Valorization Field on "Imaging agents" aims to facilitate the use of preclinical and clinical imaging for the industrial development of new imaging probes, contrast agents and radiotracers for X ray, CT, MRI, nuclear medicine, ultrasound and optical imaging. We will focus particularly on clinical applications in the fields of diagnostics, biomarkers, therapeutics and theranostics.

Context: The strategic valorization unit on imaging agents has established a roadmap for public-private R&D, including priorities and opportunities for transferring to industry:

- Develop the prospective analyses, identify the new opportunities and/or markets
- Bringing out innovative projects with aimed at industrial applications
- Mapping the environment and of the intellectual property / Analysis of the patent portfolio
- Mapping of the industries and analysis of the national and international industrial context
- The research landscape, its operators and its centers of excellence on a national and international level
- Analysis of the dynamics of the targeted markets,
- Analysis of the regulatory constraints

Action: We are currently listing all imaging agents' projects from French academia research units that have a patent application owned by a member of the alliance AVIESAN and that have demonstrated a pharmacological efficacy through a robust preclinical proof of concept.

If your imaging agent project meets those criteria, please contact sabin.carme@aviesan.fr

Oral presentation

Investigation of astatine chemistry in solution

J. Champion¹, F. Bassal², A. Sabatié-Gogova³, T. Ayed², E. Renault², J. Pilmé⁴, F. Réal⁵, C. Alliot³, D.C. Sergentu^{1,2}, N. Guo², R. Maurice¹, D. Deniaud², Z. Asfari⁶, N. Galland², G. Montavon¹

¹ SUBATECH, UMR CNRS 6457, IN2P3, Université et Ecole des Mines de Nantes, 4 rue A. Kastler, 44307 Nantes, France.

² CEISAM, UMR CNRS 6230, Université de Nantes, 2 Rue de la Houssinière, 44322 Nantes, France

³ CRCNA U892, IRTUN, 8 quai Moncousu, BP 70721 Saint Herblain, France; ARRONAX, 1, rue Aronnax, 44817 Saint Herblain, France.

⁴ Laboratoire de Chimie Théorique, UMR CNRS 7616, Université Pierre et Marie Curie, 4 place Jussieu, 75252 Paris, France.

⁵ PhLAM, UMR CNRS 8523, Université de Lille 1, Bat P5, Avenue Paul Langevin, 59655 Villeneuve d'Ascq, France.

⁶ IPHC UMR 7178, 25 Rue Becquerel, F-67087, Strasbourg Cedex, France.
champion@subatech.in2p3.fr

Objectives: Astatine 211 (At-211) is of considerable interest in nuclear medicine as a radiotherapeutic agent in view of targeted alpha therapy. It is well recognized in the community that the current lack of basic studies on At chemistry hinders the development of its therapeutic use¹. A wide research program aiming to explore the fundamental properties of At and to improve its labelling has started in Nantes.

Methods: Due to the availability of only minute amounts of At-211 produced in cyclotrons (typically 10⁻¹³ to 10⁻⁹ g are obtained by irradiation of a bismuth target), we rely on a multi-disciplinary approach combining radiochemistry, analytical chemistry and molecular modelling. Computational chemistry is to date the main and almost exclusive tool, to gain insight at the molecular level into the chemistry of this “invisible” element. Experimentally, At reactivity was investigated using a competition method founded on distributions between two distinct phases.

Results: Our methodology enabled us to determine a Pourbaix diagram (Eh/pH diagram) for At in non-complexing acidic aqueous media. In addition to the expected At⁻ species, the existence of two stable cationic forms has been evidenced, in which At appears in the oxidation states +I and +III (At⁺ and AtO⁺)². The AtO⁺ species may be used for binding At to boron cages, and subsequently to biomolecule carriers³. The complexation of AtO⁺ with different organic and inorganic ligands has been studied to obtain equilibrium constants. These investigations highlighted the peculiarity of the AtO⁺ behaviour and its ability to form covalent bonds.

Conclusion: Original trends for the rational design of new At complexes are determined.

¹ D. S. Wilbur, *Nat. Chem.* **2013**, 246–246.

² J. Champion *et al*, *J. Phys. Chem. A* **2010**, 576–582 & *J. Phys. Chem. A* **2013**, 1983–1990.

³ D. S. Wilbur *et al*, *Bioconjugate Chem.* **2012**, 409–420

Oral presentation

Radiolabelling and evaluation of [^{68}Ga]PIB derivatives for Alzheimer's disease diagnostic

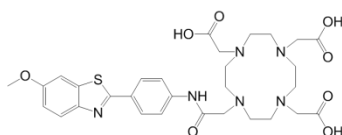
Cressier, Damien¹; Cao Pham, Thang Trang¹; Martins, André²; Jakab Toth, Eva²; Barré, Louisa¹

¹ Cyceron CEA/DSV/I2BM/ISTCT/UMR6301, Université de Caen Basse Normandie, Laboratoire de Développements Méthodologiques en Tomographie par Emission de Positons, Caen, France

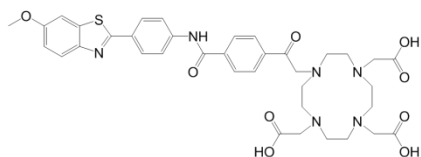
² Centre de Biophysique Moléculaire, CNRS, Orléans, France

cressier@cyceron.fr

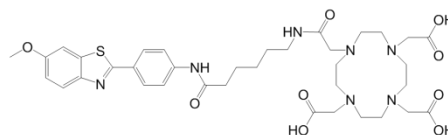
Objectives: Three analogues of the [^{11}C]PIB (AML1-3) have been developed to introduce a DOTA group in which gallium-68 was complexed. *In vivo* stability and biodistribution of [^{68}Ga]AML1-3 have been evaluated in C57Bl6 mice.



AML1



AML2



AML3

Methods: Gallium-68 was provided from a novel $^{68}\text{Ge}/^{68}\text{Ga}$ generator developed by Nordion. Fully automated processes have been developed on a Modular Lab synthesis box. After elution of the generator, gallium-68 was pre-concentrated and purified on a cation-exchange column (Strata XC). Elution of the Strata column afforded free gallium-68 which was used for the optimization of AML1-3 complexation parameters (reaction time, precursor amounts...). Then, the crude mixture was purified on C18 cartridge or HPLC column and formulated in physiological saline.

The biodistribution and the brain uptake of each radiotracer were evaluated by dissection at 30 and 60 min after injection. Brain and blood samples were analyzed by HPLC to determine the *in vivo* stability for 60 min.

Results: Fully automated and reproducible productions of [^{68}Ga]-AML1-3 have been developed. [^{68}Ga]-AML1 and [^{68}Ga]-AML3 were obtained in 20 min with C18 column purification without a total elimination of the labeling precursor in contrast to [^{68}Ga]-AML2 which was isolated by HPLC in 60 min. The radiochemical yields (decay corrected) were 46%, 57% and 12% respectively with a radiochemical purity >99%.

In vivo stability studies indicate that all the three compounds were stable in blood and brain.

Biodistribution studies show that about 0.2% (DI/g tissue) of the radiolabeled compounds cross the blood brain barrier (BBB).

Conclusion: Stability and crossing of the BBB are encouraging results to evaluate these radiotracers on a mouse model of Alzheimer's disease.

Oral presentation

Chemical delivery system of tracers to the central nervous system (CNS)

Gourand, Fabienne¹, Patin, Delphine¹, Ibazizène, Méziane¹, Dhilly, Martine¹, Levacher, Vincent², Barré, Louisa¹

¹ CEA, I²BM, LDM-TEP, UMR 6301 ISTCT, Université de Caen Basse-Normandie, GIP Cyceron, F-14074 Caen, France

² LCOFH, UMR 6014, IRCOF, CNRS, Université et INSA de Rouen, F-76130 Mont Saint Aignan, France
gourand@cyceron.fr

Objectives: [¹²³I]/[¹³¹I]metaiodobenzylguanidine (MIBG) is widely used for scintigraphic imaging studies of adrenergic tumors. As MIBG does not cross the blood brain barrier (BBB), Gourand and coll have successfully used a chemical delivery system (CDS), based on Bodor's CDS, to achieve its central nervous system penetration. MIBG has been linked to a lipophilic 1,4-dihydroquinoline carrier that enables the transport across the BBB where an oxidation followed by an enzymatic cleavage leading to the release of MIBG (Fig 1). After labeling with carbon-11 of CDS-MIBG, the *in vivo* evaluation has shown a moderate BBB penetration. The aim of the present study was to develop a series of novel CDS-MIBG to improve the BBB crossing (Fig 2).

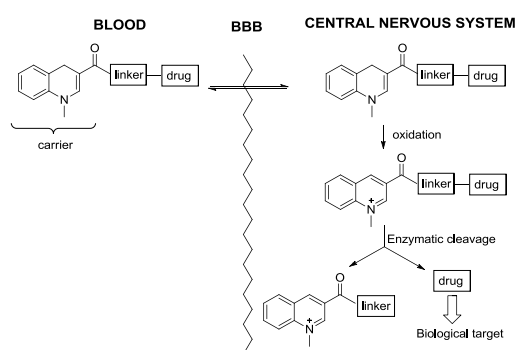


Figure 1: Bodor's Chemical Delivery System

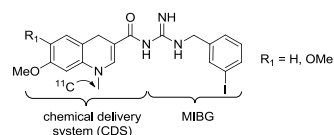


Figure 2: Structure of novel CDS-MIBG

Methods: The CDS-MIBG used as reference compounds were synthesized from corresponding 3-quinoline carboxylic acids by coupling reaction with MIBG followed by methylation and reduction steps. The radiolabelling of [¹¹C]CDS-MIBG were performed as a one-pot two step procedure by quaternarization with [¹¹C]methyl triflate followed by reduction with 1-benzyl-1,4-dihydronicotinamide (BNAH).

Results: The radiosyntheses were performed using TRACERLab FX-MeI and FX-M synthesizers. After HPLC purification and formulation, [¹¹C]CDS-MIBG were obtained in 50 min with 12- 22% decay-corrected yield based on [¹¹C]methyl triflate. After injection into rats, the results have shown a good stability of [¹¹C]CDS-MIBG in the peripheral system with a moderate BBB penetration.

Conclusion: An efficient automated synthesis of [¹¹C]CDS-MIBG has been developed. In order to improve the BBB passage, the synthesis of novel CDS-MIBG series will be undertaken with the introduction of a linker between the CDS and the MIBG.

Oral presentation

Synthesis of 4-([¹⁸F]fluoromethyl)piperidines for PET imaging

Massaba Keita, Sébastien Schmitt, Cécile Perrio*

*LDM-TEP, ISTCT, UMR 6301 CNRS, CEA, Université de Caen – Basse Normandie, CYCERON, France
perrio@cyceron.fr*

Hypothesis/Objectives. 4-(Fluoromethyl)piperidines are valuable molecular frameworks for drug discovery programs targeting central nervous system disorders and cancers. Therefore, the development of original 4-([¹⁸F]-fluoromethyl)piperidine containing radiopharmaceuticals is useful for PET imaging. In order to access to these structures, we examined the nucleophilic attack of [¹⁸F]fluoride with a series of various N-substituted 4-(halogeno- or sulfonyloxymethyl)piperidines. We postulated that such a reaction could occur either via a classical SN2 reaction or via an intramolecular quaternarization of the piperidine nitrogen followed by a ring opening of the resulting bridged bicyclic quaternary ammonium salt to give the corresponding piperidine products and/or the pyrrolidine derivatives. For a complete investigation, we studied fluorination reactions under both non-radioactive and radioactive conditions. We also performed mechanistic studies including theoretical calculations at the B3LYP/6-311+G** level to characterize all the involved intermediates and transitions states and to calculate their activation energies.

Methods. Radiofluorination reactions were carried out from K[¹⁸F]F/K222 complex in acetonitrile or DMSO at 50-180°C. Fluorinations were achieved under similar conditions using TBAF, KF or KF/K222.

Results. Starting N-Boc, N-phenyl and N-acylpiperidines led exclusively to the corresponding fluoromethylpiperidines in satisfactory yields (50-60%) and radiochemical yields (60-75%) under smooth conditions (90°C). From N-alkylpiperidines, fluorinations failed whereas radiofluorinations were efficient (> 80%) when performed above 125°C. In the latter case, a mixture of 4-([¹⁸F]-fluoromethyl)piperidines and 3-([¹⁸F]-fluoroethyl)pyrrolidines was obtained. Calculations of activation energies for the transition states corresponding to the formation of pyrrolidine and piperidine products were in accordance with the experimental results.

Conclusion. The radiofluorination of 4-(halogeno- or sulfonyloxymethyl)piperidines was efficient and general. The mechanistic pathway was function of the nature of the substituent on the piperidine ring. Extension of this approach to access to radiopharmaceuticals is underway.

Oral presentation

In the way to the quest of "the ideal" [^{18}F]-radiotracer targeting tumor neoangiogenesis: from the chemistry to the imaging of $\alpha_v\beta_3$ integrins in melanoma tumors

Magali Szlosek-Pinaud¹, Eric Amigues¹, Jürgen Schulz², Séverine Brillouet³, Sandrine Silvente-Poirot³, Eric Fouquet¹, Frédéric Courbon³, Philippe Fernandez²

¹ ISM, UMR-CNRS 5255, Groupe Synthèse-Molécules Bioactives, Université de Bordeaux

² INCIA, UMR-CNRS-5287, Université de Bordeaux

³ CRCT, UMR-INSERM-1037, Université Paul Sabatier, Toulouse

m.szlosek@ism.u-bordeaux1.fr

Objectives: The emergence of antiangiogenic therapies requires the development of specific medical imaging. $\alpha_v\beta_3$ integrin is a marker of tumor neoangiogenesis ; it binds specifically RGD (-Arg-Gly-Asp-) containing peptides. Among a variety of different radiolabeled RGD-peptides, [^{18}F]galacto-RGD,⁴ has allowed to detect $\alpha_v\beta_3$ -expressing tumors, such as melanomas, in patients.⁵ However, its radiosynthesis, remains problematic, making large-scale clinical studies challenging. To circumvent this shortcoming, we have envisaged to rethink the initial synthesis in order to use a one-step method for a site specific ^{18}F -labeling. Then, the potential of our radiotracers for PET, using tumor model, has to be evaluated, to select the "ideal" candidate for clinical studies.

Methods: A convergent synthesis of ^{18}F -labeled RGD derivatives was envisaged, using both advantages of "click chemistry" and of a ^{18}F -fluorination applying the silicon-based building blocks strategy,⁶ done on a commercially available automate (TRACERLab Fx_{F-N}[®], Ge Healthcare). The ^{18}F -mono-cycloRGD has been injected intravenously into C57black/6 mice (n = 12) bearing subcutaneous B₁₆F₁₀ melanoma xenografts. PET/CT have been realized on a clinical imager (Discovery ST, General Electrics, Milwaukee, US) and images were collected after 75min.

Results: ^{18}F -mono-cycloRGD was obtained,⁷ with higher RCY (17% (n= 4) not decay corrected) and RSA (180 GBq/ μmol) than any $\alpha_v\beta_3$ integrin tracers already in clinical trials. Furthermore, preliminary preclinical results are very promising, showing a significant uptake in tumor along with a tumor-to-

⁴ R. Haubner, B. Kuhnast, C. Mang, W.A. Weber, H. Kessler, H.J. Wester, M. Schwaiger, [^{18}F]Galacto-RGD: Synthesis, Radiolabeling, Metabolic Stability, and Radiation Dose Estimates, *Bioconjug. Chem.*, Vol. 15, pp. 61-69, 2004.

⁵ A. J. Beer, R. Haubner, M. Sarbia, C. Mang, M. Goebel, S. Luderschmidt, A. L. Grosu, O. Schnell, M. Niemeyer, H. Kessler, H.J. Wester, W.A. Weber, M. Schwaiger, Positron Emission Tomography Using [^{18}F]Galacto-RGD Identifies the Level of Integrin $\alpha_v\beta_3$ Expression in Man, *Clin. Cancer. Res.*, Vol. 12, pp. 3942-3959, 2006.

⁶ a) L. Mu, A. Höhne, P.A. Schubiger, S.M. Ametamey, K. Graham, J.E. Cyr, L. Dinkelborg, T. Stellfeld, A. Srinivasan, U. Voigtman, U. Klar, *Angew. Chem. Int. Ed.* Vol. 47, pp.4922-4925, 2008. b) A. Höhne, L. Mu, M. Honer, P.A. Schubiger, S.M. Ametamey, K. Graham, T. Stellfeld, S. Borkowski, D. Berndorff, U. Klar, U. Voigtman, J.E. Cyr, M. Friebe, L. Dinkelborg, A. Srinivasan, Synthesis, *Bioconjug. Chem.*, Vol. 19, pp.1871-1879, 2008. c) J. Schulz, M. Szlosek-Pinaud, P. Fernandez, E. Fouquet, Chemistry, *Chem. Eur. J.*, Vol. 17, pp 3096-3100, 2011.

⁷ E. Amigues, J. Schulz, M. Szlosek-Pinaud, P. Fernandez, S. Silvente-Poirot, S. Brillouet, F. Courbon, E. Fouquet, *ChemPlusChem.*, Vol. 77, pp. 345-349, 2012.

Oral presentation

background ratio of 6.1 ± 1.5 , allowing a clear identification of the tumor. However, a first evaluation of the biodistribution has shown a gastro intestinal early elimination.

Therefore, a di-cycloRGD, Si-H precursor, was prepared, starting from a glycerol-tripodal template.

Conclusion: Thanks to chemical optimizations, ^{18}F -cycloRGD-tracers could be obtained very efficiently. The preclinical studies demonstrate the reproducible ability of the ^{18}F -mono-cycloRGD to identify B₁₆F₁₀ melanoma. ^{18}F -fluorination of di-cycloRGD and further preclinical investigations are underway.

Oral presentation

A novel radiotracer to image alpha 7 by PET, the [^{18}F] FP321

Vercouillie Johnny¹, Routier Sylvain², Chicheri Gabrielle¹, Ouach Aziz², Bodard Sylvie¹, Suzenet Franck², Pin Frédéric², Mothes Céline³, Jean-Bernard Deloye³, Chalon Sylvie¹, Guilloteau Denis¹
vercouillie@univ-tours.fr

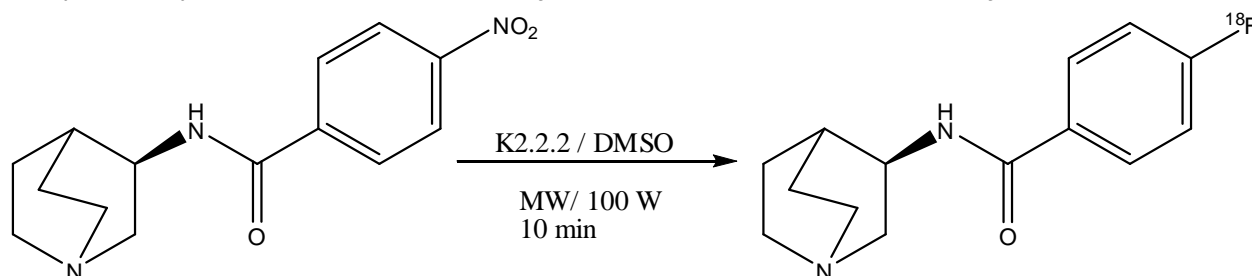
1. Université François Rabelais, Inserm U 930, CHRU, Tours, France ;

2. ICOA, Université d'Orléans, Pôle de Chimie, Orléans, France¹

3. Cyclopharma Laboratoires. Biopôle Clermont-Limagne, 63360 Saint-Beauzire, France

Objectives: The $\alpha 7$ nicotinic acetylcholine receptors (nAChRs) are ligand-gated Ca^{2+} channels composed of homopentamers of $\alpha 7$ subunits. It has been shown that $\alpha 7$ nAChRs play a role in various brain disorders such as neurodegenerative diseases, neuroinflammation, schizophrenia and depression. We report here the radiosynthesis and the preliminary biological evaluation of [^{18}F] FP321 with the aim to get a suitable $\alpha 7$ nAChRs PET radioligand

Methods: [^{18}F] *N*-[(3*R*)-1-azabicyclo[2.2.2]oct-3-yl]-4-fluorobenzamide was prepared by nucleophilic substitution starting from the correspondent nitro precursor. Two approaches were evaluated, thermal heating (165 °C for 20 min) and microwave assisted reaction (100 W for 10 min). [^{18}F] FP321 was purified by HPLC and formulated with injectable ethanol/0.9% NaCl :1/9 for injection in rats.



Cerebral biodistribution was performed in male Wistar rats separated in two groups, control and pretreated by 1 mg/kg of the $\alpha 7$ nAChR antagonist methyllycaconitine (MLA). Animals received an i.v. injection of 4 ± 1 MBq of [^{18}F] FP321 and were sacrificed 1 hour post injection. Biodistribution was assessed by measuring radioactivity uptakes (%ID/g) in blood and several brain tissues.

Results: The ^{18}F incorporation by conventional heating was low (2%). The use of microwave improved the yield up to 10% (decay corrected). Unfortunately, under microwave, concomitant to ^{18}F incorporation appears a degradation of the precursor and without degradation fluorinated tracer. Biodistribution showed a low and homogenous accumulation of the tracer (around 0.03%ID/g) in the different studied brain regions (cerebellum, striatum, hippocampus, hypothalamus and cortex). Moreover this accumulation was almost identical in the control and MLA groups.

Conclusions: We prepared a new fluorinated PET tracer, [^{18}F] FP321, to visualize $\alpha 7$ nAChRs by PET. Unfortunately, [^{18}F] FP321 displays a very low brain uptake and present a high non-specific binding. [^{18}F] FP321 will not be a suitable radiopharmaceutical to image *in vivo* $\alpha 7$ nAChRs by PET.

Research Support: ANR Malz Minalpha 7, **ANR-11-LABX-18-01**, the Région Centre and FEDER "Radex" programs

Oral presentation

Imaging tumor matrix microenvironment by PET with a fluorinated heparin sulfate mimetic

Vercouillie Johnny¹, Chicheri Gabrielle¹, **Arlicot Nicolas¹**, SiñerizFernando², Prenant Christian¹, Serriere Sophie¹, Papy-GarciaDulce³, Duval Stéphanie¹, Barritault Denis², Guilloteau Denis¹.

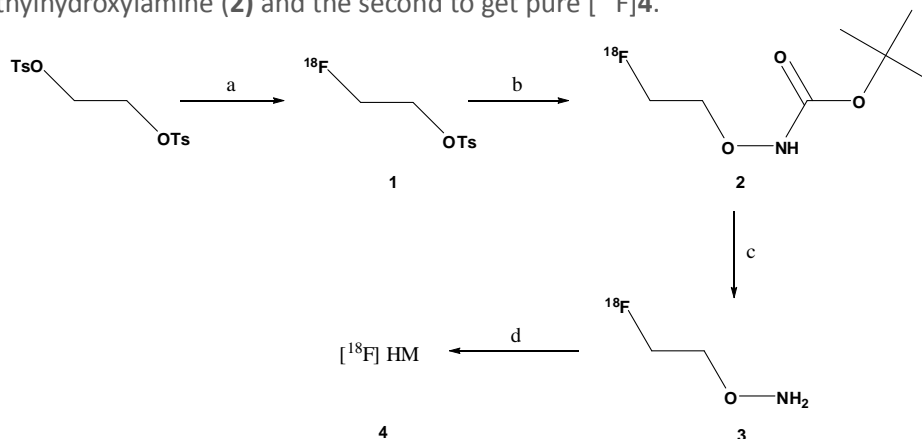
1. Université François Rabelais, Inserm U 930, CHRU, Tours, France

2. OTR3, Paris, France.

3. UPEC, EAC7149, Créteil, France.

Objectives: In order to develop a radiopharmaceutical to visualize the extracellular matrix of tumor microenvironment by PET, a polymer sugar-based compound has been used. The structure core was a Heparan Sulfate Mimetic (HM) as they mimic heparin sulfate functions and was resistant to human endogenous glycanases degradation. We developed a new ¹⁸F synthon as well as the grafting method to the HM. The radiotracer was evaluated *in vitro*, *ex vivo* and *in vivo*.

Methods: The radiosynthesis of [¹⁸F] HM (**4**) was achieved in four steps starting from ethylene ditosylate. Two HPLC purifications were required, the first one to purify the BOC-2-[¹⁸F]fluoroethylhydroxylamine (**2**) and the second to get pure [¹⁸F]**4**.



In vitro binding studies of [¹⁸F] HM with tumor homogenate from mice xenografted with PC3-cells were performed, likewise *ex vivo* biodistribution was achieved on the same animal model. Animals were sacrificed at 3 different times after radiotracer injection (10, 60 or 120 min). Several organs were removed, weighted and radioactivity was counted. μ PET experiments were also conducted in that animal tumoral model for which 34.3 ± 12.3 MBq of [¹⁸F] HM were dispensed and then scanned four hours after injection.

Results: Complete radiosynthesis was achieved in $130 \text{ min} \pm 10 \text{ min}$ and afforded (**4**) in 1.5-3.6 % decay corrected yield. *In vitro* evaluation shown that [¹⁸F] HM seems to be able to bind to matrix protein and this, specifically. Nevertheless, the biodistribution and *in vivo* experiments demonstrated a tiny accumulation of the radiotracer in the tumor.

Conclusions: We were able to prepare [¹⁸F] HM and to perform reproducible radiosyntheses through the development of a new fluorinated agent, [¹⁸F]fluoroethylhydroxylamine (**3**). This agent could be used to label macromolecules as well as low molecular weight compounds.

Poster

Ex vivo characterization of transthyretin cardiac amyloidosis (TTR-CA) using an amyloid β specific PET imaging agent. Preliminary data

Arlicot N¹, Ben-Azzouna R², Vercouillie J¹, Algalarrondo V⁴, Capron F³, Slama MS⁴, Guilloteau D¹, Le Guludec D²

¹Université François Rabelais de Tours, Inserm U930, CHRU de Tours, Tours, France

²Université Paris Diderot–Paris 7, U698 INSERM, Paris, France

³Pitié Salpêtrière, AP-HP, Paris, France

⁴Antoine Bécère, AP-HP, Paris, France

nicolas.arlicot@univ-tours.fr

Objectives: Familial amyloid polyneuropathy is a hereditary form of amyloidosis due to a mutated variant of transthyretin (TTR) produced by the liver. Cardiac involvement is characterized by extracellular depositions of amyloid β (A β) which can lead to heart failure, conduction disturbances, arrhythmias and sudden death. While early diagnosis of Transthyretin cardiac amyloidosis (TTR-CA) has important therapeutic and prognostic impact, there is no sensitive and quantitative tool to document the location and extent of cardiac A β in these patients. So we aimed to test *ex vivo* the usefulness of ¹⁸F-AV45, a high specific A β PET tracer recently FDA approved in Alzheimer's disease.

Methods: Binding of ¹⁸F-AV45 to A β was evaluated by autoradiography in myocardial tissue obtained from patients who underwent cardiac transplantation either for TTR-CA, or ischemic heart failure (controls). Frozen heart sections (20 μ m-thickness, n=2 for each data point) were incubated with ¹⁸F-AV45 at concentrations of 1 or 3nM. Nonspecific binding was assessed by incubation of adjacent sections in the presence of an excess (300 μ M) of cold AV45. After the film was developed, images were scanned and analysed by grey-level semi-quantification process using β vision+ software.

Results: ¹⁸F-AV45 uptake was significantly higher in TTR-CA myocardial sections when compared to controls (+70% \pm 10%). The intensity of ¹⁸F-AV45 binding markedly decreased in sections incubated with unlabeled AV45 (-83% \pm 5%), strongly suggesting A β specificity.

Conclusions: These preliminary data demonstrate ¹⁸F-AV45 capability to bind specifically A β in heart tissue, and provide the basis for a clinical trial designed to determine its diagnostic potential in TTR-CA patients.

Poster

Radiation dosimetry of [^{18}F]DPA-714, a potential PET biomarker for neuroinflammation

Arlicot N¹, Chalon S¹, Vercouillie J¹, Santiago-Ribeiro M-J¹, Bodard S¹, Serrière S¹, Guhlan Z¹, Stabin M², Kassiou M³, Guilloteau D¹

¹Université François Rabelais de Tours, Inserm U930, CHRU de Tours, CIC-IT 806, Tours, France,

²Vanderbilt University, Nashville, TN,

³Brain and Mind Research Institute, Sydney, NSW, Australia

Objectives: The translocator protein 18kDa (TSPO), minimally expressed in healthy brain, is up-regulated in pathological conditions, coinciding with microglial activation. It is thereby an early and sensitive in vivo biomarker for molecular imaging of neuroinflammation. Therefore, the development and validation of efficient radiopharmaceuticals targeting TSPO is a major challenge for the diagnosis and therapeutic monitoring of brain diseases. Knowledge of the dosimetry in humans is a key step in the validation of such radiopharmaceuticals. We aimed to estimate from biodistribution data in mice the radiation dosimetry of the positron emission tomography (PET) TSPO radioligand [^{18}F]DPA-714.

Methods: Biodistribution data performed in Swiss mice by iv injection of [^{18}F]DPA-714 (2 MBq/100 μL) were used for the prediction of radiation dosimetry in humans. Animals were euthanized at five different time points (5, 30, 60, 240 and 360 min post-injection), and the radioactivity in 12 organs was measured and expressed as a percentage of the injected dose per gram of tissue. These data were then extrapolated to a reference 70kg adult male phantom, and organ doses and the effective dose were calculated using the OLINDA/EXM 1.1 software.

Results: Most organs received from 1 to 20 $\mu\text{Sv}/\text{MBq}$. The adrenals, kidneys and lungs appear to receive the highest doses, about 100, 90 and 60 $\mu\text{Sv}/\text{MBq}$, respectively. The effective dose was estimated to be 17.2 $\mu\text{Sv}/\text{MBq}$.

Conclusions: This study provide a reasonable basis for predicting the approximate human dosimetry of [^{18}F]DPA-714 and suggests that it has an acceptable effective dose, consistent with published data for other common fluorine-18 radiopharmaceuticals, and compatible with the use of this new compound in subsequent clinical investigations, for evaluation by molecular imaging of neuroinflammatory processes associated with brain diseases.

Poster

Nucleophilic radiofluorination at room temperature via aziridinium

Marie Médoc, Franck Sobrio

CEA, I²BM, LDM-TEP - UMR 6301 ISTCT, CNRS, CEA, Université de Caen Basse-Normandie - GIP
Cyceron, F-14074 Caen, France
medoc@cyceron.fr

Objectives

β -fluoroamine moieties are commonly present in bioactive molecules and also in some PET radiopharmaceuticals. However, electrodonating substituents on the amine function can induce instability of precursors and involves a two-step radiosynthesis. Amines bearing electrodonating substituents lead to immediate reaction of the β -leaving group to form a reactive aziridinium intermediate. Those aziridiniums have been observed during fluorination of β -aminoalcohols with DAST or Deoxofluor. Here, based on *in situ* aziridinium formation from β -aminoalcohols, we have developed the nucleophilic radiolabelling of β -[¹⁸F]fluoroamines in one radioactive step at room temperature (RT).

Methods: The preparation of the aziridinium and their fluorination with common fluorine sources used in radiochemistry were validated and optimized using the model compound *N,N*-dibenzylphenylalaninol. Aziridiniums were prepared from β -aminoalcohol precursors before to react with [¹⁹F]- or [¹⁸F]-fluoride. Incorporation yield of [¹⁸F]-fluorine was determined by radio-TLC and the identity of the products was established by HPLC coelution with the non-radioactive standard compound.

Results: Aziridiniums were generated from alcohols and triflic anhydride at RT. The radiolabelling could be performed from different source of [¹⁸F]-fluoride. Two [^{18/19}F]-fluorinated regioisomers were obtained demonstrating the reaction via aziridinium intermediate. Radiofluorination yields were 58% at RT and 83% at 90°C. The best radiolabelling conditions were applied for the radiolabelling of *N*-fluoroethylamine and *N*-phenylfluoropropanamine molecules bearing *N*-benzyl, *N*-allyl or *N*-propargyl groups. [¹⁸F]-Radiolabelled compounds were obtained within good to moderate yields (14–57%).

Conclusion: We have developed a new method for the radiolabelling of β -[¹⁸F]-fluoroamines *via* aziridinium intermediates by nucleophilic substitution at RT. This method could be used for the preparation of radiopharmaceuticals by a one-step radiosynthesis with stable alcohol precursor.

Poster

Radiolabeling and *in-vivo* evaluation of multi-target-directed ligand for Alzheimer disease treatment

Fillesoye Fabien¹, Prieur Laurent¹, Ibazizene Meziane¹, Dhilly Martine¹, Hovhannisyan Narinée¹, Gourand Fabienne¹, Rochais Christophe², Dallemagne Patrick², Barré Louisa¹

¹ CEA, DSV/I2BM, LDM-TEP Group, GIP Cyceron, Bd Henri Becquerel, BP 5229, 14074 Caen Cedex, France.

² Université de Caen Basse-Normandie, EA-4258 – Centre d'Etudes et de Recherche sur le Médicament de Normandie (CERMN), F-14032 Caen, France.

fillesoye@cyceron.fr

Objectives: An interesting pharmacological approach to cure Alzheimer disease is the development of ligands with multiple targets. A virtual screening of the CERMN chemical library was carried out to find molecules able to associate an activation of 5-HT₄ receptor (5-HT₄R) and an inhibition of acetylcholinesterase (AChE). Our goal was to realize the radiolabeling with carbon-11 (¹¹C) of MR-31147, which has a good affinity both for AChE inhibition (IC₅₀=63nM) and 5-HT₄R (K_i=7nM), in order to assess their *in-vivo* potential.

Methods: The radiolabeling of [¹¹C]-MR31147 was performed using desmethylated compound with [¹¹C]CH₃OTf. The crude product was purified by HPLC and formulated into injectable solution. After intravenous injection in Wistar rats, blood and brain radiometabolism, blood-brain barrier penetration and peripheral biodistribution were evaluated at 5 and 60 min post-injection.

Results: [¹¹C]-MR31147 was obtained with a high radiochemical purity (>99%), a specific activity ranging from 6 to 14GBq/μmol and was stable over 2 hours in physiological saline with ethanol (90/10). Blood analysis revealed that 72±5% of the parent compound was recovered at 5 min and only 24±4% at 60 min. In contrast, 87±1% of [¹¹C]-MR31147 was found in the brain at 60 min. Brain uptake was 0.12±0.01%ID/g at 5 min to decrease to 0.06±0.01%ID/g at 60 min. Peripheral biodistribution studies showed rapid and high uptake in kidneys, liver and lung; at 60 min, the highest uptake was found in small intestine.

Conclusion: The radiosynthesis of [¹¹C]-MR31147 is efficient and reproducible. *In-vivo* preliminary study showed a low brain uptake with a progressive decrease. However, the compound seems to be stable in brain with no diffusion of metabolites from blood. The important uptake of the compound in the small intestine is consistent with the localisation of 5-HT₄R. These results will be completed by μPET imaging and cerebral distribution in regions of interest.

Poster

Structural analysis of opioid receptors for evaluation of [^{18}F]fluorinated derivatives of 3,4-dimethyl-4-phenylpiperidines as potential radioligands for PET imaging

Nathalie Colloc'h¹, Sébastien Schmitt², Cécile Perrio²

¹ CERVOxy, ISTCT, UMR 6301 CNRS, CEA, Université de Caen – Basse Normandie, CYCERON, France

² LDM-TEP, ISTCT, UMR 6301 CNRS, CEA, Université de Caen – Basse Normandie, CYCERON, France
colloch@cyceron.fr

Hypothesis/Objectives. The *trans*-3,4-dimethyl-4-phenylpiperidines such as LY255582, LY246736 and JDtic are an unique class of compounds exhibiting pure opioid antagonist activity that may prove useful in the treatment of obesity, psychosis and depression, as well as opioid and cocaine abuse and other central nervous system disorders. We anticipated that [^{18}F]-fluorinated derivatives of *trans*-3,4-dimethyl-4-phenylpiperidines would represent attractive radiopharmaceuticals to investigate drug addiction and associated psychiatric disorders (schizophrenia, depression) by PET imaging. We undertook to examine the suitable sites for fluorine incorporation and to develop the synthesis of fluorinated compounds.

Methods. The crystallographic structure of the complex between JDtic and the kappa opioid receptor (KOR) has been used to examine the suitable site for fluorine incorporation. Synthesis of the fluorinated compounds was based on a diastereoselective multistep procedure with the methylation of a metallocenamine generated from 4-aryl-3-methyl-1,2,3,6-tetrahydropyridine as the key reaction to afford the (3R*,4S*)-form.

Results. The analysis of the crystallographic structure of the complex between JDtic and KOR revealed that the methyls on position 3 and 4 of the 3,4-dimethyl-4-phenylpiperidines are perfectly suitable for a fluorination since they are not engaged in any kind of interaction with the opioid receptor.

Conclusion. Derivatives of 3,4-dimethyl-4-phenylpiperidines bearing a fluorine atom on the methyl groups at positions 3 or 4 should fit in the KOR active site. In particular, fluorinated analogues of JDtic should then bind to KOR with the same order of affinity and specificity than JDtic. Preparation and *in vitro* evaluation of fluorinated analogues of opioid antagonists for a further radiolabeling with fluorine-18 are underway.

Poster

Discovery of novel $\alpha 7$ -nAChR ligands : from an idea to in rodent results for ^{18}F TEP imaging.

Frédéric Pin,¹ Johnny Vercouillie,² Aziz Ouach,¹ Emilie Bertrand,¹ Sylvie Mavel,² Zuhail Gulhan,² Gabrielle Chicheri,² Jean-Bernard Deloye,³ Denis Guilloteau,² Franck Suzenet,¹ Sylvie Chalon² and Sylvain Routier¹

¹ Institut de Chimie Organique et Analytique, Université d'Orléans, UMR CNRS 7311, Orléans Cedex, France.

² Université François Rabelais, Inserm U 930, CHRU, Tours, France ;

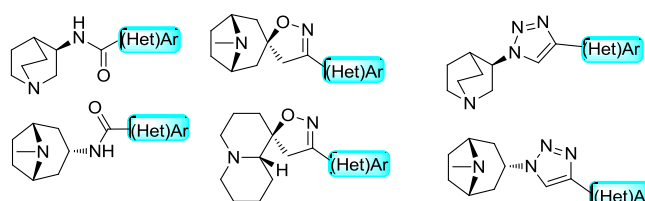
³ Laboratoires Cyclopharma, Tours, France

Sylvain.routier@univ-orleans.fr

Hypothesis: The neurotransmitter acetylcholine (ACh) exerts its effects on the central nervous system (CNS) through two distinct muscarinic mAChRs and nicotinic nAChRs receptors types: nAChRs belong to the superfamily of ligand-gated ion channels possessing a pentameric structure.¹ Because of their distribution and abundance in the CNS (in particular in the hippocampus and cortex), the $\alpha 7$ subtypes are potential diagnosis and therapeutic targets for brain disorders that involve these cerebral regions. In this field, $\alpha 7$ nAChR agonists were identified and allowed the design of novel therapeutic agents for Alzheimer Disease (AD). Having in hand a human compatible [^{18}F]-labeled positron emission tomography (PET) tracer to realize the early diagnostic or to validate the efficiency of therapies in clinical trials for AD is indubitably crucial. In this aim, we also envisioned to design novel $\alpha 7$ nAChR ligands and their transformation into a [^{18}F] PET tracer.

Methods: Synthesis, molecular modelling and in vitro evaluation of each final compound were also associated to create a complete consortium able to identify the best ligands. Radiolabelling and in vivo evaluation determine the brain penetration as well as the tracer potency of drug.

Results: In this aim, based on our expertise in heterocyclic bio-mimetic development,² we also obtained a wide library of novel $\alpha 7$ nAChR ligands and some of them were transformed into [^{18}F] PET tracer. Ligands contain a quinuclidine, a tropane or a 8H-quinolizine moiety. We present herein chemistry,³ SAR studies, molecular modelling docking studies which confirmed the binding mode of the developed ligands, *in vitro* efficiency (SAR), radiolabeling and *in vivo* results in rats.



Poster

Conclusion

We present herein chemistry,³ SAR studies, molecular modelling docking studies which confirmed the binding mode of the developed ligands, in vitro efficiency (SAR), radiolabeling and in vivo results in rats.

References

- 1 J. Wu, M. Ishikawa, J. Zhang and K. Hashimoto *Int. J. Alzheimers Dis.*, **2010**, 2010, 11; F. Dajas-Bailador and S. Wonnacott., *Trends Pharm. Sci.*, **2004**, 25, 317. C. Gotti, M. Zoli and F. Clementi, *Trends Pharm. Sci.*, **2006**, 27, 482; D. Paterson and A. Nordberg, *Prog. neurobiol.*, **2000**, 61, 75.
- 2 C. Neagoie, E. Vedrenne, F. Buron, J. Y Merour, S. Rosca, S. Bourg, O. Lozach, L. Meijer, B. Baldeyrou, A. Lansiaux and S. Routier, *Eur. J. Med. Chem.* **2012**, 49, 379; R. Boulahjar ; A. Ouach, M. Chiurato, S. Bourg, M. Ravache, R. Le Guével, S. Marionneau-Lambot, T. Oullier, O. Lozach, L. Meijer, C. Guguen-Guillouzo, S. Lazar, M. Akssira, Y. Troin, G. Guillaumet and S. Routier, *J. Med. Chem.*, **2012**, 55, 9589;
- 3 Routier, S. ; Suzenet, F. ; Pin, F. ; Chalon, S. ; Vercouillie, J. ; Guilloteau, D. **WO 2012143526** ; F. Pin, J.Vercouillie, A. Ouach, S. Mavel, Z. Gulhan, G. Chicheri, C. Jarry, S. Massip, J.-B. Deloye, D. Guilloteau, F. Suzenet, S. Chalon S. Routier, *Org. biomol. Chem.* **2013**, submitted.

Research Support:ANR Malz MInAlpha 7,the Labex Iron (**ANR-11-LABX-18-01**), the Région Centre and Cyclopharma Laboratories.

Keywords: CH Arylation, thiazolotriazoles, palladium catalysis, radiolabeling, TEP imaging.

Oral presentation

Absorbed doses estimations for patients with B-acute lymphoblastic leukemia treated by radioimmunotherapy ^{90}Y -epratuzumab tetraxetan

Ludovic Ferrer^{1,3}, Thomas Eugene², Nicolas Varmenot^{1,3}, Thomas Carlier^{2,3}, Françoise bodéré^{2,3}

¹ ICO René Gauducheau, ST Herblain, France

² CHU Nantes, France

³ CRCNA U892, Nantes, France

ludovic.ferrer@ico.unicancer.fr

Objectives: The aim of this study is to present estimated absorbed doses for B-acute lymphoblastic leukaemia patients treated with 2 fractions of ^{90}Y labelled antiCD22 Epratuzumab tetraxetan.

Methods: 6 acute leukaemia patients (4 men, 2 females) were enrolled in a radio-immunotherapy clinical trial in Nantes University hospital. The injection regimen consisted of 2 infusions: the first was a co-infusion of ^{90}Y (3 patients: 92.5 MBq/m², 3 patients: 185 MBq/m²) and ^{111}In labelled (185 MBq) epratuzumab while the second consisted of a single ^{90}Y labelled epratuzumab injection. 5 whole-body scans and tomographic images were acquired to assess absorbed doses to organs such as lungs, liver, spleen, and kidneys. Red marrow (RM) absorbed dose was assessed with imaging and blood samples. Absorbed doses to organs for the second fraction were extrapolated from first fraction estimations.

Results: Median organs absorbed doses were 0.4, 1.5, 0.8, 2.8, 3.7, 2.4, 2.1, 3.7 mGy/MBq for whole-body, right and left lungs, liver, spleen, right and left kidneys and RM respectively. Liver and spleen normalized absorbed doses as well as both kidneys absorbed doses were linearly correlated ($R^2=0.81$, $p<0.01$ and $R^2=0.66$, $p=0.02$ respectively). As patients suffered from a lymphoblastic disease, it was hard to highlight any correlation between RM absorbed doses and patient haematological toxicities.

Conclusion: A dosimetric study was performed on B-acute lymphoblastic leukaemia patients. A strong correlation was exhibited between liver and spleen normalized absorbed doses as both organs present a large amount of blood.

Oral presentation

Boosted selective internal radiation therapy (B-SIRT) using 90Y-loaded glass microspheres induces prolonged overall survival for PVT patients

Garin E ^{1,2,3}, Lenoir L ^{1,2}, Edeline J ^{3,4}, Laffont S ^{2,3}, Boucher E ^{3,4}, Rolland Y ⁵.

¹ University of Rennes 1, F-35043, France

² Department of Nuclear Medicine, Cancer Institute, Rennes, F-35042, France

³ INSERM U991, Rennes, F-35033, France

⁴ Department of Oncology, Cancer Institute, Rennes, F-35042, France

⁵ Department of Radiology, Cancer Institute, Rennes, F-35042, France

e.garin@rennes.unicancer.fr

Objectives: Evaluation of the response rate and survival of hepatocellular carcinoma PVT patients treated with TheraSphere® using the boost or intensification concept.

Methods: TheraSphere® was administered in 41 PVT hepatocellular carcinoma patients (main= 13, lobar = 22, segmental= 6). MAA SPECT/CT quantitative analysis was used for the calculation of the tumour dose (TD), the healthy injected liver dose (HLD) and the injected liver dose (LD). Intensification (increase of the injected activity with the goal to achieve a TD> 205Gy with a LD > 150 Gy and a HLD<120Gy) was used for patients with a TD< 205 Gy. Response was evaluated at 3 months using EASL criteriae. OS was evaluated using Kaplan and Meyer tests.

Results: Mean 90Y-loaded microspheres injected activity was 3.1±1.5 GBq. Mean LD was 143±49Gy. With a threshold TD of 205Gy, MAA-SPECT/CT was predictive of response with a sensibility of 100%, and an overall accuracy of 90% (0FN, 4FP). Knowing the TD and the HLD, 41.5% of the patients received an intensification of the with a good response rate (85%) and without increased liver grade III toxicity (6.2% as against 12.5% in the non boosted patients, ns). Ten patients were downstaged or in CR, 5 received a lobar hepatectomy. Median OS was 18months [12-27]. It was 7.5m [12-27] for patients with a TD<205Gy versus 18m [12-28.5] for patients with a TD>205Gy, p=0.018. OS was 15m [3-∞] for patients with main PVT versus 21.5m [12-28.7] for patients segmental or lobar PVT (ns). Finally Os was 21.5m for patients with a TD>205Gy and a good PVT targeting (n= 36).

Conclusion: Boosted selective internal radiation therapy using 90Y-loaded glass microspheres induces prolonged overall survival for PVT patients without increasing liver toxicity.

Oral presentation

Collapsed cone superposition for radionuclide dosimetry: implementation and validation for ^{90}Y therapy

Manuel Sanchez-Garcia¹, Isabelle Gardin², Rachida Lebtahi¹, Arnaud Dieudonné¹

¹ *Department of Nuclear Medicine, Beaujon Hospital, Assistance Publique-Hôpitaux de Paris (APHP), Clichy, France*

² *Department of Nuclear Medicine, Henri Becquerel Cancer Center and Rouen University Hospital, & QuantIF – LITIS [EA 4108], Rouen, France*
Manuel.Sanchez.Garcia@outlook.com

Objectives As an alternative to Monte Carlo (MC) simulations, a collapsed cone superposition (CC) algorithm has been developed to speed up the computation of absorbed dose (AD) in ^{90}Y therapy, taking tissue heterogeneities into account.

Methods CC computes dose using a ^{90}Y point kernel generated in water medium with the MCNP MC code. This kernel is scaled by radiological distance between source and destination voxels in order to account for tissue heterogeneities. Validation was performed against MCNP for semi-infinite sources corresponding to the 6 interface combinations involving soft tissue, lung and bone. Comparisons to MC were performed in terms of relative AD difference (ΔAD) in low gradient regions (LGR) and distance to agreement (DTA) in high gradient regions (HGR). Additional validation was performed for 2 clinical cases, corresponding to simulations of an intravascular liver treatment with a lung shunt (case 1) and a bone metastasis treatment in a lumbar vertebra (case 2). Both cases were compared to MC in terms of DVHs and average AD to organs ($\overline{\text{AD}}$).

Results For the semi-infinite source, ΔAD in LGR was below 1.5%. DTA in HGR was below 0.5 mm, except for the bone-lung interface, where it reached 0.8 mm. For clinical case 1, $\overline{\text{AD}}$ differed by 1.6, 0.4 and 0.5% in lung, non-tumoral liver and the tumor respectively. DVHs differed by less than 1.1%. For case 2, $\overline{\text{AD}}$ differed by 0.3 and 0.1% in the vertebra and bone marrow respectively. DVHs differed by less than 0.6%. Calculation times were below 8 minutes on a single processor for CC and 40 hours on a 40 nodes cluster for MC (10^8 histories).

Conclusion Our results show that the CC absorbed dose computation for ^{90}Y therapy agrees well with MC on heterogeneous media, while greatly reducing computation times, making CC a promising algorithm for radionuclide dosimetry.

Oral presentation

Development of a fully 3D Monte Carlo Reconstruction method for Preclinical PET with Iodine-124 (ReS_PET): efficiency in heterogeneous media

Matthieu Moreau^{1,2}, Nicolas Chouin², Françoise Kraeber-Bodéré^{1,3}, Michel Chérel¹ and Thomas Carlier^{1,3}

¹ CRCNA, INSERM, Université de Nantes, UMR_S 892, Nantes, France

² LUNAM Université, ONIRIS, "AMaROC", Nantes, France

³ CHU Nantes, Service de Médecine Nucléaire, Nantes, France
matthieu.moreau@oniris-nantes.fr

Hypothesis : In pre-clinical 3D PET imaging, iodine-124-based acquisition for quantitative purpose is always a challenge due to the complex decay scheme of this isotope and the relative long positron range. The objective of this study was to tackle this issue by developing a fully Monte Carlo (MC) LOR-OSEM reconstruction method, called ReS_PET.

Methods: The system matrix (SM), required in iterative reconstruction, was pre-calculated with MC methods taking into account the native symmetries of the system.

Three MC SM were computed: PSF modelling only (SM2), PSF + iodine-124 in water (SM3), PSF + iodine-124 in heterogeneous media (SM4). A ray-tracing Siddon algorithm was also developed (SM1) for comparison.

Three heterogeneous media (P1 to P3) with water, lungs and bones were simulated, with hot (contrast 4:1) and cold (contrast 0:1) regions filled with iodine-124.

Activity was inserted in all media for P1 and only the regions composed of water were filled for P2 and P3.

For P1, the contrast recovery coefficients (C_Hot and C_Cold) in water and the ratio (R) between hot region in lung and water were calculated.

For P2 and P3, profiles relative to five regions were plotted in order to assess the combination of contrast recovery coefficient and spatial resolution.

Results: For P1, C_Hot was 130%, 107%, 107%, 98% and C_Cold was 45%, 67%, 93%, 98% with SM1 to SM4 respectively. R was 0.92 with SM4 while it was less than 0.33 with other SM.

Additionally, when the accuracy of system matrix increased, the contrast recovery coefficients were higher, for all regions for P2 and P3.

Conclusion: This work showed that for a given noise level, the use of an accurate SM with a realistic detector response and physical effects in the object was essential for achieving a high quantitative accuracy as compared with SM computed with a geometrical model.

Oral presentation

Comparative study of tomographic reconstructions algorithms for dosimetry purposes

Henri Der Sarkissian^{1,2}, Marie-Paule Garcia³, Daphnée Villoing³, Ludovic Ferrer⁴, Jeanpierre Guédon¹, Manuel Bardès³

¹ LUNAM Université, IRCCyN UMR CNRS 6597, Polytech Nantes

² KEOSYS, Saint-Herblain

³ UMR 1037 INSERM/UP, Centre de Recherche en Cancérologie de Toulouse

⁴ ICO René Gauducheau, Saint-Herblain

henri.dersarkissian@univ-nantes.fr

Hypothesis: Dosimetry is a major challenge in nuclear medicine both for radioprotection and targeted treatment assessment. Clinical dosimetric computation relies on a series of image processing steps as well as accurate quantitative imaging. The goal of this paper is to assess and quantize the sensibility of dosimetry according to image reconstruction algorithms for 3D nuclear imaging.

Methods: TestDose is a Monte Carlo based simulation tool for generation of dosimetric problems. This software, developed in INSERM UMR 892 and INSERM UMR 1037, is used to generate the study data. We emphasize that such simulation-generated data is advantageous over real patient data since can we intrinsically design and know the exact structural and dosimetric ground truth.

Our digital virtual setup models ¹¹¹In-octreoscan studies acquired with GE Infinia SPECT. 60 projection views over 180 degrees rotation extent of digital NCAT phantom are generated for each temporal frame.

In the next step, the projection views are reconstructed into 3D+t volumes. A variety of tomographic reconstruction algorithms are used for inter-patient comparison: analytic algorithms (FBP with various filters) and iterative (ART, SART, OSEM). Moreover, we decided to include newly developed algorithms based on the Mojette transform, a discrete geometry exact version of the Radon transform.

Finally, each different set of reconstructed volumes is used for clinical dosimetry assessment at voxel and VOI scale.

Results: By design, this virtual study allows the computation of *ground truth* dosimetry from the input NCAT phantom data. This result is obtained by Monte Carlo simulation using GATE software.

The comparison between manually performed dosimetry and the obtained ground truth finally reveals discrepancies and introduced by each tomographic reconstruction algorithm.

Conclusion: We designed a virtual protocol for dosimetry accuracy assessment with respect to tomographic reconstruction algorithms. Quality of these algorithms is assessed against objective clinical measure.

Poster

Evaluation of 2 registration softwares based on ITK for dosimetric estimations in molecular radiotherapy.

Matthieu Gillet¹, Ludovic Ferrer^{2,3}, Nicolas Varmenot^{2,3}, Henri Der Sarkissian¹, Jeanpierre Guedon¹

¹ Ecole Polytechnique, Nantes, France

² ICO René Gauducheau, ST Herblain, France

³ CRCNA U892, Nantes, France

ludovic.ferrer@ico.unicancer.fr

Objectives: To assess absorbed doses to normal organs or tumours, several imaging sessions are needed in order to estimate the amount disintegrations occurring in patient's emission sources. Thus, images should be registered against each other to evaluate the radiopharmaceutical time evolution in all pixels of patient's volume. The aim of this work was to evaluate two 3 dimensional registration softwares based on Insight Toolkit (ITK) library: one developed in our institution and one freely available.

Methods: ITK is an open-source, cross platform library that provides developers with an extensive suite of algorithms for image analysis and especially registration. We developed a command line tool to perform 3D rigid registration based on well-known algorithms such as Mattes mutual information and multi-resolution approaches. Elastix is an open-source software based on ITK that allows for rigid and non-rigid registrations. To compare our development against Elastix, we acquired CT scans of Liqui-fil™ phantom. Known displacements (table 1) were performed on acquired images in order to evaluate software capabilities. Moreover, Liqui-Fil™ phantom contains fillable moving organs allowing for evaluating Elastix non-rigid registration.

Results: In all cases, rigid registrations performed by Elastix were slightly better and faster than those achieved by our application. For non-rigid transformations, Elastix was able to visually correct for most of displacements introduced in Liqui-Fil™ organs. Further investigations are still needed to quantify resultant misalignment.

Conclusion: ITK library was used to develop a rigid registration application. This software was compared to Elastix a software toolkit for rigid and non-rigid registration. For rigid registration, Elastix presented better performances than our own application.



LIST OF PARTICIPANTS



Last name	First name	Institute	Country	e-mail
ABADIE	Jérôme	Oniris	France	jerome.abadie@oniris-nantes.fr
ANSQUER	Catherine	CHU Nantes	France	catherine.ansquer@chu-nantes.fr
ARLICOT	Nicolas	CHU Tours	France	nicolas.arlicot@univ-tours.fr
ATZORI	Véronica	Bayer Healthcare	France	veronica.atzori@bayer.com
AVILA	Sébastien	AAA	France	sebastien.avila@adacap.com
BAILLY	Clément	CHU Nantes	France	baillyclement@hotmail.fr
BAILLY	Matthieu	CHU Tours	France	matthieu.bailly@orange.fr
BAKA	Irini	Athens Hospital	Greece	irini_baka@hotmail.com
BARBET	Jacques	Arronax	France	Jacques.Barbet@univ-nantes.fr
BARRE	Louisa	Cyceron	France	barre@cyceron.fr
BATRAK	Olga	Arronax	France	batrak@arronax-nantes.fr
BEAUPERE	Nicolas	CRCNA	France	beauperenicolas@yahoo.com.au
BEHAR	Ghislaine	CRCNA	France	ghislaine.behar@univ-nantes.fr
BENDRIEM	Bernard	Siemens Healthcare	USA	bernard.bendriem@siemens.com
BENOIT	Jean-Pierre	MINT	France	jean-pierre.benoit@univ-angers.fr
BERNAUDIN	Myriam	Cyceron	France	bernaudin@cyceron.fr
BERTHAUD	Maxime	CRCNA	France	maxime.berthaud@inserm.fr
BERTRAND	Emilie	ICOA	France	emilie.bertrand@univ-orleans.fr
BODEI	Lisa	IEO	Italy	lisa.bodei@ieo.it
BODET-MILIN	Caroline	CHU Nantes	France	cbodetmilin@gmail.com
BOIARYNA	Liliana	ICOA	France	liliana.boiaryna@univ-orleans.fr
BOUDOUSQ	Vincent	CHU Nimes	France	vincent.boudousq@chu-nimes.fr
BOURDEAU	Cécile	Arronax	France	bourdeau@arronax-nantes.fr
CAO	Liji	Inviscan	France	liji@inviscan.fr
CARLIER	Thomas	CHU Nantes	France	thomas.carlier@chu-nantes.fr
CARME	Sabin	AVIESAN	France	sabin.carme@aviesan.fr
CHAKHOYAN	Ararat	Cyceron	France	ararat.chakhoyan@gmail.com
CHALON	Sylvie	UFR Tours	France	sylvie.chalon@univ-tours.fr
CHAMPION	Julie	Subatech	France	champion@subatech.in2p3.fr
CHEREL	Michel	CRCNA	France	Michel.Cherel@univ-nantes.fr
CHOUIN	Nicolas	Oniris	France	nicolas.chouin@oniris-nantes.fr
CIAVATTI	Laurent	Isotop4life	France	laurent.ciavatti@univ-nantes.fr
CIKANKOWITZ	Annabelle	MINT	France	annabelle.cikankowitz@etud.univ-angers.fr
COLLOC'H	Nathalie	Cyceron	France	colloch@cyceron.fr
COQUERY	Nicolas	INRA ADNC	France	nicolas.coquery@rennes.inra.fr
CORROYER-DULMONT	Aurélien	Cyceron	France	corroyer@cyceron.fr
COUTURIER	Olivier	CHU Angers	France	ocouturier70@me.com
CRESSIER	Damien	Cyceron	France	cressier@cyceron.fr
DAVODEAU	François	CRCNA	France	davodeau@nantes.inserm.fr
DEGRAEF	Marie	CHU Nantes	France	marie.degraeef@univ-nantes.fr
DERRIEN	Aurélié	CHU Poitiers	France	derrien.aurelie@gmail.com
DESEVEDAVY	Stéphanie	CRCNA	France	Stephanie.Desevedavy@inserm.fr
DIAB	Maya	CRCNA	France	maya.diab@univ-nantes.fr
DIEUDONNE	Arnaud	APHP Beaujon	France	arnaud.dieudonne@bjn.aphp.fr
DORSO	Laëtitia	Oniris	France	laetitia.dorso@univ-nantes.fr
DUVAL	Elise	Nucleopolis	France	elise.duval@nucleopolis.fr
EUGENE	Thomas	CHU Nantes	France	thomas.eugene@chu-nantes.fr

Last name	First name	Institute	Country	e-mail
FAIVRE-CHAUVET	Alain	CRCNA	France	Alain.Faivre-Chauvet@univ-nantes.fr
FANTINO	Frédéric	Spectrum	France	spectrumfrance@gmail.com
FERRER	Ludovic	CHU Nantes	France	ludovic.ferrer@ico.unicancer.fr
FILLESOYE	Fabien	Cyceron	France	fillesoye@cyceron.fr
FRINDEL	Mathieu	CRCNA	France	mathieu.frindel@univ-nantes.fr
GARCION	Emmanuel	MINT	France	emmanuel.garcion@univ-angers.fr
GARIN	Etienne	CEM Rennes	France	e.garin@rennes.unicancer.fr
GASCHET	Joëlle	CRCNA	France	joelle.gaschet@univ-nantes.fr
GAUGLER	Marie-Hélène	CRCNA	France	marie-helene.gaugler@inserm.fr
GERIN	Pascal	GE Healthcare	France	pascal.gerin@ge.com
GESTIN	Jean-François	CRCNA Isotop4life	France	jean-francois.gestin@inserm.fr
GOGUET	Thierry	GE Healthcare	France	Thierry.Goguet@ge.com
GORIN	Jean-Baptiste	CRCNA	France	jean-baptiste.gorin@univ-nantes.fr
GOUARD	Sébastien	CRCNA	France	sebastien.gouard@univ-nantes.fr
GOURAND	Fabienne	Cyceron	France	gourand@cyceron.fr
GUEDON	Jeanpierre	Polytech	France	jeanpierre.guedon@polytech.univ-nantes.fr
GUILLOTEAU	Denis	CHU Tours	France	denis.guilloteau@univ-tours.fr
GUIRAUD-CAIZERGUES	Nathalie	Spectrum	France	spectrumfrance@icloud.com
GUO	Ning	Subatech	France	ning.guo@subatech.in2p3.fr
HINDRE	François	MINT	France	francois.hindre@univ-angers.fr
HOVHANNISYAN	Narinée	Cyceron	France	hovhannisyann@cyceron.fr
IBISCH	Catherine	Oniris	France	catherine.ibisch@oniris-nantes.fr
JACOBS	Andreas	EIMI	Germany	ahjacobs@uni-muenster.de
KAFROUNI	Hanna	Dosisoft	France	kafrouni@dosisoft.fr
KALICHUK	Valentina	CRCNA	France	valentina.Kalichuk@etu.univ-nantes.fr
KRAEBER-BODERE	Françoise	CHU Nantes	France	francoise.bodere@chu-nantes.fr
KREUTEL	Sven	Raytest	France	sven.kreutel@raytest.com
KUHNAST	Bertrand	CEA	France	bertrand.kuhnast@cea.fr
LEBTAHI	Rachida	APHP Beaujon	France	rachida.lebtahi@bjn.aphp.fr
LEFAUCHEUR	Jean-Luc	Inviscan	France	jeanluc@inviscan.fr
LEGENDRE	Claire	MINT	France	claire_legendre@yahoo.fr
LELAN	Faustine	CRCNA	France	faustine.lelan@univ-nantes.fr
LEOST	Françoise	CGO	France	francoise.leost@univ-nantes.fr
LE SAEC	Patricia	CRCNA	France	patricia.lesaec@univ-nantes.fr
MAGNEN	Mélia	Oniris	France	melia.magnen@etu.univ-nantes.fr
MALBERT	Charles-Henri	INRA ADNC	France	Charles-Henri.Malbert@rennes.inra.fr
MATHIEU	Cédric	CHU Nantes	France	cedric.mathieu44@gmail.com
MATOUS	Etienne	CRCNA	France	etienne.matous@univ-nantes.fr
MAURICE	Rémi	Subatech	France	remi.maurice@subatech.in2p3.fr
MENAGER	Jérémie	CRCNA	France	jeremie.menager@univ-nantes.fr
MERNY	Thibault	Lemer Pax	France	event@lemerpax.com
MEROUANI	Djamila	CRCNA	France	djamila.merouani@univ-nantes.fr
MONTAVON	Gilles	Subatech	France	montavon@subatech.in2p3.fr
MOREAU	Matthieu	CRCNA	France	matthieu.moreau@oniris-nantes.fr
MORIO	Floriane	Oniris	France	floriane.morio@oniris-nantes.fr
MOURATOU	Barbara	CRCNA	France	barbara.mouratou@univ-nantes.fr
OUYA	Olivier	Bayer Healthcare	France	olivier.ouya@bayer.com
OYEN	Wim	Nijmegen Med Centre	The Netherlands	W.Oyen@nucmed.umcn.nl

Last name	First name	Institute	Country	e-mail
PALLARDY	Amandine	CHU Nantes	France	amandine.pallardy@chu-nantes.fr
PALM	Stig	Gothenburg Univ	Sweden	stig.palm@radfys.gu.se
PECORARI	Frédéric	CRCNA	France	frederic.pecorari@univ-nantes.fr
PERRIO	Cécile	Cyceron	France	perrio@cyceron.fr
RAJERISON	Holisoa	CRCNA	France	holisoa.rajerison@inserm.fr
RAUSCHER	Aurore	CRCNA	France	aurore.rauscher@univ-nantes.fr
RODRIGUES	Nuno	ICOA	France	nuno.rodrigues@univ-orleans.fr
ROUTIER	Sylvain	ICOA	France	sylvain.routier@univ-orleans.fr
ROUSSEAU	Caroline	CHU Nantes	France	caroline.rousseau@ico.unicancer.fr
ROUSSEAU-POIVET	Julie	Oniris	France	julie.rousseau@oniris-nantes.fr
ROUSSEAUX	Olivier	Guerbet	France	olivier.rousseaux@guerbet-goup.com
SANCHEZ-GARCIA	Manuel	APHP Beaujon	France	galesko@outlook.com
SEHEDIC	Delphine	MINT	France	delphine.sehedic@gmail.com
SERгентU	Dumitru-Claudiu	Subatech	France	sergentu@subatech.in2p3.fr
SUZENET	Franck	ICOA	France	franck.suzenet@univ-orleans.fr
SZLOSEK-PINAUD	Magali	ISM	France	magali.szlosek-pinaud@u-bordeaux1.fr
TESSON	Mathias	ICS	UK	m.tesson.1@research.gla.ac.uk
THOMAS	Thierry	Bayer Healthcare	France	thierry.thomas@bayer.com
TODDE	Sergio	Tecnomed	Italy	sergio.todde@unimib.it
VALABLE	Samuel	Cyceron	France	valable@cyceron.fr
VAUCLIN	Sébastien	Dosisoft	France	vauclin@dosisoft.com
VERCOUILLIE	Johnny	UFR Tours	France	vercouillie@univ-tours.fr
VERGER	Elise	MINT	France	elise.verger@etud.univ-angers.fr



ILE BAGUENAUD 25 km

Pte Saint GILDAS 15 km

PIAGE de la BANCHE 132 km

NOIRMOUTIER 25 km